Published in final edited form as:
*J Comp Neurol*. 2010 May 1; 518(9): 1460–1499. doi:10.1002/cne.22283.

# Paraventricular hypothalamic nucleus: axonal projections to the brainstem

**Joel C. Geerling**[*], **Jung-Won Shin**[*], **Peter C. Chimenti**, and **Arthur D. Loewy**[**]
Department of Anatomy and Neurobiology Washington University School of Medicine St. Louis, MO 63110, USA

## Abstract

The paraventricular hypothalamic nucleus (PVH) contains many neurons that innervate the brainstem, but information regarding their target sites remains incomplete. Here, we labeled neurons in the rat PVH with an anterograde axonal tracer, *Phaseolus vulgaris* leucoagglutinin (PHAL) and studied their descending projections in reference to specific neuronal subpopulations throughout the brainstem. While many of their target sites were identified previously, numerous new observations were made. Major findings include: (1) In the midbrain, the PVH projects lightly to the ventral tegmental area, Edinger-Westphal nucleus, ventrolateral periaqueductal gray matter, reticular formation, pedunculopontine tegmental nucleus, and dorsal raphe nucleus. (2) In the dorsal pons, the PVH projects heavily to the pre-locus coeruleus, yet very little to the catecholamine neurons in the locus coeruleus, and selectively targets the viscerosensory subregions of the parabrachial nucleus; (3) In the ventral medulla, the superior salivatory nucleus, retrotrapezoid nucleus, compact and external formations of the nucleus ambiguus, A1 and caudal C1 catecholamine neurons, and caudal pressor area receive dense axonal projections, generally exceeding the PVH projection to the rostral C1 region; (4) The medial nucleus of the solitary tract (including A2 noradrenergic and aldosterone-sensitive neurons) receives the most extensive projections of the PVH, substantially more than the dorsal vagal nucleus or area postrema. Our findings suggest that the PVH may modulate a range of homeostatic functions, including cerebral and ocular blood flow, corneal and nasal hydration, ingestive behavior, sodium intake, and glucose metabolism, as well as cardiovascular, gastrointestinal, and respiratory activities.

### Keywords

autonomic; cardiovascular; ingestive behavior; respiratory; salt appetite; stress

## Introduction

From a biomedical perspective, the paraventricular hypothalamic nucleus (PVH) is perhaps the most important nucleus in the forebrain. Among the many subpopulations of neurons in the PVH, the most extensively studied are its neuroendocrine cells, through which the brain controls the pituitary gland. Magnocellular neuroendocrine neurons send their axons into the neurohypophysis (posterior pituitary), where in well-characterized homeostatic responses to physiologic perturbations they release either oxytocin or vasopressin (antidiuretic hormone) into the systemic circulation. Parvicellular neuroendocrine neurons, in contrast, release various signaling peptides into the median eminence. These peptides, also referred to as

[**]Correspondence to: Arthur D. Loewy, Ph.D. Dept. of Anatomy and Neurobiology- Box 8108 Washington University School of Medicine 660 S. Euclid Avenue St. Louis, MO 63110 USA Tel: 314-362-3930 Fax: 314-362-3446 loewya@pcg.wustl.edu.
[*]These authors contributed equally to this work.

releasing and release-inhibiting hormones, are carried by the pituitary portal system to the adenohypophysis (anterior pituitary), where they regulate the release of pituitary hormones that control endocrine tissues throughout the body.

In addition to these well-known neuroendocrine groups, the PVH contains a large population of neurons which send their axons to the brainstem and spinal cord (Saper et al., 1976; Swanson, 1977). Though partly interspersed with the aforementioned neuroendocrine neurons, these caudally-projecting cells form an entirely separate subpopulation (Swanson and Kuypers, 1980; Swanson et al., 1980). Along with a homologous group of neurons extending into the lateral hypothalamus, they provide a major output channel from the forebrain to the brainstem and spinal centers that regulate autonomic nervous system. Parvicellular PVH neurons in general are activated in response to a variety of stressors, both physical and psychological (Sawchenko et al., 1996; Herman and Cullinan, 1997), and those that project to the brainstem and spinal cord form a critical link between the limbic forebrain and various homeostatic and autonomic responses to stress (Blair et al., 1996; Sawchenko et al., 1996; Felder et al., 2003; Li and Patel, 2003; Thompson and Swanson, 2003; Coote, 2005; Ferguson et al., 2008).

Axonal projections from the PVH to the brainstem and spinal cord have been analyzed by a variety of tracing techniques (Saper et al., 1976; Swanson, 1977; Sawchenko and Swanson, 1982a; Luiten et al., 1985; Zheng et al., 1995; Toth et al., 1999) – as well as other reports). Here, using the anterograde axonal tracer PHAL (*Phaseolus vulgaris* leucoagglutinin), we demonstrate the sites in the rat brainstem that receive input from the PVH, a number of which were not identified or were misidentified in previous tracing studies.

Originally, these experiments were intended to evaluate simply whether axons from the PVH target a specific subpopulation of cells in the caudal medulla – the aldosterone-sensitive neurons in the nucleus of the solitary tract (NTS; see Geerling et al., 2006a; Geerling et al., 2006b). However, cases with PHAL injections in the PVH exhibited patterns of axonal labeling in other parts of the brainstem that differed substantially from previous reports. It appeared that projections from the PVH to multiple groups of neurons had been either overlooked or misinterpreted, so we re-analyzed the entire brainstem to redefine the sites innervated by this hypothalamic nucleus. In a number of anatomically complex subregions of the brainstem, we compared axonal labeling from the PVH with the distributions of various cell type-specific markers, revealing multiple target nuclei which were mislabeled in previous accounts. Based on the well-established connections and functions of some of these target neurons, the findings described below suggest that the PVH influences a larger and somewhat different set of behaviors and visceral/autonomic functions than were considered within its purview based on previous descriptions of its output connections.

## Materials and Methods

The neural tracing experiments described below were performed in male and female Sprague-Dawley albino rats (250-350g; Harlan, Indianapolis, IN). All animal procedures were approved by the Washington University School of Medicine Animal Care Committee and conformed to NIH guidelines.

### PHAL injections

In a large series of rats (n=362), PHAL (2.5% solution made in 0.02 M potassium phosphate buffer, pH 8.0; Vector, Burlingame, CA) was iontophoresed into the PVH for 20, or in some cases 30 minutes. The stereotaxic coordinates used for these injections were 0.40 mm lateral to the midline, between 1.35 and 1.60 mm caudal to bregma, and between 7.1 and 7.3 mm

deep to the dural surface. Seven days after surgery, rats were anesthetized with sodium pentobarbital (50 mg/kg, i.p.) and perfused through the aorta with 200 mL of 0.9% saline, followed by 500 mL 4% paraformaldehyde prepared in a 0.1 M sodium phosphate buffer (pH 7.4).

Brains were post-fixed at room temperature in the same solution for one or more days, until sections were cut using a freezing microtome, either 50 μm thick in the transverse plane (all injection sites, and the entire brainstem in three cases) or in select cases 200 μm in the sagittal plane (partial brainstems from four cases, used for triple-immunofluorescence labeling). Sections were stored in 0.1 M sodium phosphate buffer containing 0.1% sodium azide at room temperature until immunohistochemical staining, initiated in most cases within hours after sectioning. After examining PHAL labeling in and around the PVH in every case, select brains with restricted PHAL uptake in a sizeable population of neurons in the PVH were chosen for detailed analysis (n=7). Additional brains with injection sites surrounding and in some cases partially involving the PVH were analyzed as well, a few of which are mentioned briefly here only to confirm that the PVH itself was the focal source of axonal labeling in the brainstem sites discussed below, or to expound upon a region (the dorsolateral PAG) that is more heavily innervated by sites neighboring the PVH.

## Antisera

PHAL antisera were used from three different species. For DAB immunohistochemical labeling of injection sites in every case, and full-brain series of coronal sections from the key PVH-injected cases, we used a goat antiserum (diluted 1:20,000; product #2224, Vector, Burlingame, California). For double- and triple-immunofluorescence labeling, a rabbit polyclonal (1:7,500; product #2300, Vector) or a mouse antisera (1:700; V. Karpitskiy, St. Louis, MO) were used. The specificity of these antisera for PHAL was confirmed by the fact that neither produced any labeling in brain tissue from cases that were not injected with PHAL. Similarly, little or no axonal immunoreactivity was found in the brainstem in cases with PHAL injections that missed the PVH.

A goat polyclonal antiserum to cholera toxin β subunit (CTb; 1:25,000 dilution; product #703; List Biologicals, Campbell, CA) was used to identify retrogradely labeled neurons in the PVH following CTb injections in the NTS. This antiserum produces no labeling in tissue sections from animals that were not injected with CTb. Furthermore, CTb retrograde labeling was restricted in NTS-injected cases like the one shown below to the well-established pattern of afferents to this nucleus; sections from this case were discussed and shown in a previous study (Geerling and Loewy, 2006a).

Catecholamine neurons were labeled with an affinity-purified polyclonal antibody raised in either sheep (1:1000; product #AB1542, Chemicon) or rabbit (1:1000; product #AB152, Chemicon International; Temecula, CA) against denatured tyrosine hydroxylase (TH) from rat pheochromocytoma. TH-immunoreactive cell bodies were found only in established groups of catecholamine neurons, including a lateral subset of cells within the dorsal vagal nucleus, the A1 and A2 noradrenergic groups and C1-C3 adrenergic neurons in the medulla oblongata, A4-A7 groups in the pons, and A8-A10 dopaminergic groups in the midbrain, in exactly the same neuroanatomical pattern as our previous work using these antisera (Geerling et al., 2006b; Geerling and Loewy, 2006b; Shin et al., 2008). Adrenergic neurons were identified with a sheep polyclonal antibody against phenylethanolamine-N-methyltransferase (PNMT), which was raised against bovine PNMT (1:200; product #AB146, Chemicon). This antiserum labeled neurons in the C1-C3 groups in the medulla exclusively.

To label tryptophan hydroxylase (TrpOH, an enzyme expressed exclusively in serotoninergic neurons), we used the PH8 mouse monoclonal antibody (1:4,000; "PH8 antibody," product # MAB 5278, Chemicon). This antibody was raised against phenylalanine hydroxylase (PH) purified from monkey liver (Jennings et al., 1986). In unfixed tissue, it binds a shared epitope in PH, TH, and tryptophan hydroxylase that is relatively conserved across mammalian species including humans, rabbits and rats (Cotton et al., 1988). However, in TH this epitope is modified by formaldehyde fixation such that it no longer binds the PH8 antibody, allowing selective labeling of tryptophan hydroxylase in fixed tissue (Haan et al., 1987; reviewed in Paterson et al., 2006). In the present experiments, consistent with previous reports (Haan et al., 1987; Paterson et al., 2006)–see for other reports), this monoclonal antibody produced immunolabeling in formaldehyde-fixed brain sections only in the raphe nuclei that are known to contain serotoninergic neurons. The PH8 antibody never produced immunolabeling in regions that contained TH-expressing catecholaminergic neurons.

Choline acetyltransferase (ChAT) was labeled with an affinity-purified polyclonal antiserum raised in goat against ChAT enzyme purified from human placenta (1:500; product #AB144P, Chemicon). This antiserum selectively labels cells in the well-known distributions of cranial nerve motoneurons (III, IV, V, VII, XII) and parasympathetic preganglionic neurons (Edinger-Westphal nucleus, salivatory nuclei, ambiguus complex, dorsal vagal nucleus), and in the laterodorsal and pedunculopontine tegmental nuclei of the pons and midbrain, as well as axons emerging from each of these structures (e.g. trigeminal motor nerve root, intra-axial facial nerve, hypoglossal nerve).

The neuropeptide urocortin was labeled using a rabbit polyclonal antiserum (1:500; product #U4757; Sigma, St. Louis, MO). This antiserum was raised against a synthetic peptide corresponding to the C-terminal of human urocortin (amino acids 25-40 with N-terminally added lysine) conjugated to KLH. The immunogen sequence (human) corresponds to pro-urocortin (amino acids 105-120) and is identical in rat urocortin (manufacturer's information). The antibody was evaluated for activity and specificity by radioimmunoassay (RIA) and immunohistochemistry, and the does not cross-react with human or rat corticotrophin-releasing hormone (CRH 6-33), sheep CRH, PACAP38, human ACTH, or human ACTH18-39 (manufacturer's information). In the Edinger-Westphal (EW) nucleus, this antiserum labeled a small subset of neurons in the midline, in a distribution distinct from the ChAT-immunoreactive parasympathetic preganglionic neurons in this region.

Finally, an affinity-purified polyclonal antiserum was used to label 11-β-hydroxysteroid dehydrogenase type 2 (HSD2, #1296; Chemicon). This antiserum was raised in sheep using a synthetic protein generated from nucleotides 385-1204 of rat *hsd11b2* (Gomez-Sanchez et al., 2001). After testing a range of dilutions from 1:1,000 to 1:200,000, this antiserum was found to produce optimal signal-to-noise at a dilution of 1:40,000 for labeling the restricted group of cytoplasmic immunoreactive neurons located in the NTS (Geerling et al., 2006b). The highly restricted pattern of cytoplasmic labeling produced by this antibody in the rat brain is identical to the pattern of *hsd11b2* gene expression identified by *in situ* hybridization (Roland et al., 1995b). At higher concentrations (dilutions below ~1:20,000), this antibody also labels all neuronal nuclei in the brain. As HSD2 is tethered to the endoplasmic reticulum by a specialized N-terminal domain (Odermatt et al., 1999) and is not found in the cell nucleus (Naray-Fejes-Toth and Fejes-Toth, 1996; Naray-Fejes-Toth and Fejes-Toth, 1998), and because *hsd11b2* mRNA is extremely scarce throughout the brain in general (resulting in a complete lack of detection in original localization attempts; Roland et al., 1995a), we interpreted the ubiquitous nuclear staining at higher antibody concentrations as non-specific cross-reactivity. Western blot analysis using this antiserum labels a single band in the kidney at ~40kD, the predicted molecular weight of HSD2 (Gomez-Sanchez et

al., 2001; verified in our laboratory, unpublished observation, JCG). No labeling was obtained at any MW in tissue homogenates from whole brain, parietal cortex, or brainstem unless high antibody concentrations (1:1000) and large amounts of protein are loaded (120μg per lane), which produce additional "non-specific"-appearing bands at multiple MW, which are barely detectable above background labeling in each protein lane (C. Gomez-Sanchez, personal communication; JCG, unpublished observations). The lack of HSD2 detection in the brainstem by western blot may be due to the paucity of HSD2-expressing cells in this tissue (~500-1000 neurons total in the NTS, among millions of non-expressing neurons throughout this region of the CNS) relative to the kidney. For further details regarding HSD2 immunoreactivity in the rat brain see (Geerling et al., 2006b).

### Immunohistochemical protocols

Single-labeling for either CTb or PHAL was performed using the ABC-DAB histochemical technique. First, the primary antibody was diluted in a solution containing 0.3% Triton-X (Sigma) and 5% donkey serum in 0.1 M sodium phosphate buffer (pH = 7.4) with 0.1% sodium azide. Sections were incubated overnight at room temperature on a rotary shaker, then washed in potassium phosphate buffered saline (KPBS; 0.01M, pH = 7.4), transferred to a biotinylated donkey anti-goat secondary antibody solution (1:200; Jackson ImmunoResearch, West Grove, PA) diluted in the same solution used for the primary antiserum, then washed in KPBS, incubated in the avidin-biotin complex for 1h (ABC, Vectastain kit, Vector Labs, Burlingame, CA), washed in KPBS, and colorized in diaminobenzidine for 5-10 min. (DAB, 1 tablet, 1 tablet urea, 15 ml distilled water, #D-4418; Sigma). Sections were then washed in KPBS, mounted on gelatinized glass slides, air-dried, counterstained with 0.1% thionin (pH = 4.6), and coverslipped.

Double- and triple-immunofluorescence labeling was performed using standard immunofluorescence protocols. Thick (200 μm) sagittal sections were incubated for 4h in a 1% solution of Triton X-100 in KPBS prior to permeablize the tissue prior to incubation in primary antisera. Sections were incubated overnight (50 μm transverse sections) or 40-48h (200 μm sagittal sections) in a mixed solution of two or three primary antisera diluted in the same PBS solution containing 5% donkey serum and Triton X-100 described above. After two 5 min washes in KPBS, sections were transferred for 2-3h into a mixture of two or three secondary antibodies raised in donkey against mouse, rabbit, sheep, or goat conjugated to Cy2, Cy3, or Cy5 (each diluted 1:500; all from Jackson). Sections were then washed, mounted on gelatin-coated glass slides, air-dried, coverslipped atop a fade-retardant glycerol solution containing *n*-propyl gallate and sodium azide, and secured around the edges using fingernail polish prior to confocal imaging with oil objectives

### Confocal and brightfield imaging

Brightfield images were taken using a CCD camera and Nikon ACT-1 software (v2.62). Image cropping, resizing, and adjustments in brightness, contrast, sharpness, and color balance were performed using Adobe Photoshop CS.

All confocal imaging was performed with an Olympus Fluoview FV500b laser-scanning microscope. Most large montage images were acquired as multiple individual stacks using a 20x oil objective (NA 1.17) in 1 μm z-steps through the full thickness of the tissue section – either 50 μm transverse or 200 μm sagittal sections. Next, 30-40 z-frames (transverse sections) or 90-120 z-frames (thick sagittal sections) were collapsed into a two-dimensional, maximum-projection image to produce individual tiles (642 × 642 μm) each at a resolution of 1024 × 1024 pixels (thus one pixel in the X-Y plane, the minimum unit of resolution, covers roughly 0.6 × 0.6 μm). Finally, individual 2D projection images were aligned into large-area photomontages using Adobe Photoshop, with adjustments in brightness and

contrast as necessary. Individual image stacks from a minority of thick sections exhibiting unusually high levels of background labeling or noise were median-filtered (radius = 2) in MetaMorph or Photoshop. Certain high-magnification inset images were acquired using a 60x oil objective (NA 1.4) in 0.5 μm z-steps. Any mention of “appositions” or “close contacts” in the following text reflects an observation verified by examination of individual optical planes through the parent stack, not simply an impression from a two-dimensional projection shown in one of the figures here.

All manipulations of confocal stacks and z-frame projections were performed using MetaMorph software (Molecular Devices, Sunnyvale, CA, USA). Pseudocoloration of these images and uniform brightness and contrast adjustments were performed in Photoshop. All illustrations were prepared using Adobe Illustrator CS by drawing in separate layers atop either a brightfield photomicrograph or a confocal montage (combined from maximum projections of individual confocal stacks, as described above) with frequent reference to the original tissue sections and original confocal stacks to resolve any uncertainties present in these two dimensional images.

### Terminology

The terms “close contact” and “apposition” are used in certain parts of this article to indicate a PHAL-labeled bouton (generally 1-3 μm in diameter) immediately adjacent to a cell body or dendrite labeled with some other marker in any three-dimensional direction (either apposed within the X-Y plane in one or more single optical sections or at the same X-Y location in one or more z-planes directly atop or beneath a labeled structure, i.e. immediately in front of or behind it in the z-axis) with no unlabeled pixels between the two structures for at least one pixel-width of contact. Determining whether a point of contact between a bouton and presumed post-synaptic site forms a synapse requires electron microscopic analysis, so it is not within the purview of the present dataset to determine whether any points of contact represent actual synapses. These appositions, or close contacts, simply represent sites where synapses may exist and in some cases where electron microscopic analysis could provide useful information in the future.

## Results

### PVH projection to the NTS

To best target our anterograde tracer injections, we first analyzed the distribution of PVH neurons that project to the brainstem. Figure 1 shows retrograde neuronal labeling in the PVH after injecting a tracer into the NTS, which receives by far the most extensive input from the PVH. This pattern of retrograde labeling resulted from a large injection of CTb (cholera toxin, β-subunit) centered in the caudal medial NTS and involving adjacent parts of the area postrema and dorsal vagal nucleus (case #8148, see inset Figure 1A').

Using Swanson's nomenclature for the PVH (Swanson, 1998), we found the greatest concentration of labeled neurons that project to the NTS in the medial parvicellular PVH subdivision (PVH-mp), followed by lesser amounts in the dorsal parvicellular (PVH-dp), lateral parvicellular (PVH-lp), and forniceal (PVH-f) subdivisions. A few labeled small to medium-sized neurons were present in the PVH magnocellular subdivision (PVH-M), which is probably not the result of spurious uptake of blood-borne CTb at the neurohypophysis – the site where magnocellular PVH and supraoptic neurons terminate – since no comparable cell body labeling was seen in the supraoptic hypothalamic nucleus (SON). The lateral hypothalamic area contained some neurons that project to the NTS (Fig. 1F). These cells were continuous rostrally with the retrogradely labeled neurons in the caudal parts of the PVH-lp and PVH-f and exhibited similar morphology, suggesting that they may belong to

the same basic population. More caudally, the dorsomedial hypothalamic nucleus contained fewer CTb-labeled neurons, but none of the PHAL cases used in this report had injections that encroached on this region.

## PHAL injection sites

Seven rats had PHAL injections involving the PVH-mp. Case #2223 was selected as the optimal experiment because its injection site maximally involved the PVH-mp (Fig. 2). The distribution of PHAL labeled PVH neurons correlated well with the pattern of retrogradely labeled neurons seen in this nucleus after a CTb injection in the NTS (Fig. 1). Photoimages comparing these two cases are presented in Figure 3.

The other PHAL cases had injection sites centered mainly in the PVH-mp with varying involvement of the PVH-dp. None of the cases had injections solely restricted to either the PVH-mp or PVH-dp. Case #2276 were centered mainly in the PVH-mp with slight involvement of the PVH-dp and PVH-lp (not shown), while Case #2221 had an injection in the PVH-dp, with some spillage into the caudal PVH-mp (Fig. 10A). None of our experiments had injections confined to the PVH-lp or PVH-f.

## PHAL axonal labeling in the brainstem

Figure 4 presents a series of drawings showing the PVH axonal projections to the brainstem (Case #2223).

In the rostral midbrain (Fig. 4A) at the level of the superior colliculus, two groups of labeled axons were seen. The first group coursed near the cerebral aqueduct in the central gray matter, with few apparent branches or boutons. A minority of these fibers entered the Edinger-Westphal nucleus (EW), forming with a highly limited number of boutons with either the urocortin-immunoreactive centrally-projecting EW neurons or the cholinergic parasympathetic preganglionic EW neurons. The second and larger group of labeled axons coursed dorsolaterally between the substantia nigra and the medial lemniscus, traveling primarily dorsal to the dopaminergic (TH-immunoreactive) cells in this region without branching or terminating, except for a moderate terminal field in a medially adjacent subregion of the ventral tegmental area located just rostral and lateral to the entrance of the fasciculus retroflexus into the interpeduncular nucleus.

In the caudal midbrain at level of the inferior colliculus (Fig. 4B), PHAL-labeled axons in the central gray matter formed a moderately dense terminal field encompassing the ventrolateral subdivision of the periaqueductal gray (PAGvl) and dorsal raphe nucleus primarily ipsilateral to PHAL injection. PHAL-labeled boutons in the dorsal raphe appeared to exhibit a preferential relationship with TH-immunoreactive cells belonging to the dorsal-caudal A10 group of dopaminergic neurons (A10dc, Supplemental Figure). A small number of fibers extended dorsally into the lateral and dorsolateral PAG, but these formed few apparent branches or boutons. Many fibers coursed ventrolaterally from the PAGvl, increasingly so at more caudal levels, to join the other major group of axons, which continued dorsally and caudally past the substantia nigra and into the midbrain reticular formation (MRF). Most labeling in this region appeared to represent fibers of passage oriented in a dorsomedial (fibers arriving from the ventrolateral midbrain) or ventrolateral (fibers departing the PAGvl) direction, although a modest amount of scattered branching and bouton formation was apparent throughout, roughly comparable to that found in the PAGvl and dorsal raphe. Many of these axons surrounded or permeated a group of large dopaminergic neurons in the MRF (the A8 dopaminergic neurons of the retrorubral field; their location is outlined Fig. 4B based on TH-immunofluorescence from an adjacent

section), but we could find at best minimal evidence for appositions between PHAL-labeled axons and the catecholamine neurons here (see Supplemental Figure).

In the pons (Fig. 4C & D), the combined fiber bundles from the PAG and ventral midbrain coursed through the MRF and pedunculopontine tegmental nucleus (not shown) in association with the superior cerebellar peduncle into the dorsolateral pons. A dense terminal field targeted the lateral parabrachial nucleus (PBl), and was concentrated in three regions: external lateral, central lateral, and dorsal lateral PB subnuclei (Fig. 4C). Further caudally, a moderate number of fibers coursed around and through a PB region that has been termed “waist area” of the PB (PBwa) that is embedded in the superior cerebellar peduncle (Fig. 4D) and ventral to the gustatory region of the PB towards a terminal field in a dorsomedial segment of the medial PB subnucleus (PBm) located just dorsal to the mesencephalic trigeminal nucleus and tract (MeV) (Fig. 4D). Medial to and intermingled with MeV neurons, a highly dense terminal field was found immediately rostral and ventral to the locus coeruleus (LC), in the pre-locus coeruleus (pre-LC) (Figs. 4D, 5 & 6A).

The distinction between the heavy PVH input to the pre-LC and its limited projection to the LC is shown in a series of coronal sections and a sagittal section through this region co-labeled for PHAL and TH in Figures 5 and 6A, respectively. Only a few fibers of passage were found coursing through the core of the LC (Fig. 5), and even the perinuclear plexus of TH-labeled dendrites, most of which extend rostrally and ventromedially from the LC core, overlapped minimally with the peripheral field of varicose axons terminating in the pre-LC. Only a small number of potential contacts between PHAL-labeled boutons and TH-labeled structures were apparent in this region, consistent with previous electron microscopic observations (Reyes et al., 2005). Similarly, this cluster of PHAL-labeled axons exhibited little or no relationship with neurons extending caudally from the laterodorsal tegmental nucleus, and no labeling was found ventromedial to the pre-LC in other areas of the periaqueductal gray matter (Fig. 4C&D), such as Barrington's nucleus (pontine micturition center) other than a few fibers of passage.

From the PB/pre-LC region, labeled fibers turned sharply in a ventral direction, coursing lateral to and through the trigeminal motor nucleus. They continued caudally in the pontine reticular formation with little or no apparent branching until terminating in the superior salivatory nucleus (SSN) (Fig. 4E & F). Axonal labeling in a sagittal section of the SSN is shown in Figure 6B, demonstrating that a dense axon terminal field envelops a cluster of small cholinergic neurons just rostral to the facial nucleus, with only minimal axonal labeling in the underlying A5 noradrenergic cell group

At nearby levels of the rostral medulla, a restricted plexus of axons arborized along the floor of the fourth ventricle and extended ventrally in the midline, following the distribution of the C3 adrenergic neurons (Fig. 4F). This terminal field originated at least in part from a small contingent of fibers that continued from the midbrain on a periventricular course without entering midbrain or pontine reticular formation.

Many fibers from the rostral medullary reticular formation extended under and around the facial nucleus towards the ventral medullary surface, where they densely innervated a thin stripe of tissue extending from roughly the level of the SSN back through the dorsolateral funiculus of the spinal cord. In the coronal plane, the most extensive arborization of labeled axons near the ventral medullary surface targeted a region ventromedial to the facial nucleus called the retrotrapezoid nucleus (RTN, Fig. 4F). This enormous plexus of axons formed numerous *en passant* boutons along its entire course. Although the greatest density of fibers was in line with the retrotrapezoid nucleus, just lateral to the parapyramidal region, some axonal labeling did extend as far medially as the pyramidal tract. Occasional close contacts

were found on some of the serotoninergic neurons found in this region (not shown), but this did not appear to be a dense input.

In the medulla, most fibers remained in the reticular formation and either turned dorsomedially towards the rostral NTS (described below) or continued ventrally to target structures in the ventrolateral medulla (Fig. 4G-J). In the ventrolateral medulla, three major groups of neurons received substantial input from the PVH: the nucleus ambiguus (NA), the C1/A1 column of adrenergic and noradrenergic neurons, and the caudal pressor area (CPA). The axonal labeling in these regions is presented in a series of sagittal sections shown in Figure 7.

Within the nucleus ambiguus, the compact formation (NAc) received by far the densest input. Many PHAL-labeled boutons enveloped the ChAT-ir neurons in this compact, longitudinally-arranged group. These results are illustrated in Fig.8A in a sagittal section and in the coronal sections of Fig. 9A & B. Significantly less axonal labeling was present in the semi-compact (NAsc) and loose (NA-L) formations, despite some examples to the contrary, such as the dorsally-oriented ChAT-immunoreactive dendrite of a NA-L neuron shown at the top part of Figure 9C. Interestingly, a dense cluster of varicose axons was usually found in the intermediate reticular formation lying dorsal to the NA and caudal to the NAc, slightly outside the extent of ChAT-ir dendrites that extend dorsally from the NAsc or NA-L (Fig. 4H). Outside the area of these large NA motoneurons, many smaller ChAT-ir neurons in the external formation (NAex = parasympathetic preganglionic neurons) were targeted by clusters of PHAL-labeled varicose axons. This relationship is illustrated in consecutive sagittal sections through this region in Figure 7, and depicted in the coronal plane in Figure 9D.

Varicose axons were found throughout the entire extent of the C1/A1 catecholamine cell column (Figs. 7 & 8B). Within roughly 500 μm caudal to the facial motor nucleus, the rostral C1 adrenergic neurons were associated with a moderate density of input from the PVH (Fig 8C). Caudally, where these neurons collect into a more compact column dorsal to the lateral reticular nucleus (the C1/A1 transition zone) (Fig. 9C), PHAL-labeled axons formed a more concentrated terminal field, which continued in association with the A1 noradrenergic neurons extending caudally to the cervical spinal cord. Almost no axonal labeling was found in the vicinity of pre-cerebellar neurons in the lateral reticular nucleus itself (Figs 4I, 4J, & 7), or the territory between the NA column and catecholamine neurons, which contains the ventral respiratory column (BötC, pre-BötC, rVRG, and cVRG; Fig. 7).

In the caudal medulla, this axon terminal field extended laterally from the A1 neurons beginning at levels just rostral to the pyramidal decussation and continuing into the cervical spinal cord. This dense axon terminal field enveloped a region extending to the medullary surface, where some fibers merged with those coursing caudally from the retrotrapezoid nucleus. This region, ventrolateral to the A1 group, corresponds to the caudal pressor area (CPA), a functionally-identified pressor region that spans the medullo-cervical junction (Gordon and McCann, 1988; Sun and Panneton, 2002; Seyedabadi et al., 2006; Iigaya et al., 2007). The CPA received one of the densest projections found in the entire brainstem, less only than what was present in the NTS and pre-LC region. There is currently no specific marker for CPA neurons (Seyedabadi et al., 2006), so we illustrated this region in greater detail in Figure 10 using case #2221, which exhibited the densest CPA axonal labeling in our series of PVH experiments, resulting from an injection centered in the PVH-dp (Fig. 10A).

Outside this region of the ventrolateral medulla, the overwhelming majority of PHAL-labeled axons coursed through the reticular formation towards the dorsomedial medulla.

Before entering the NTS, many of these axons branched, forming occasional boutons within the reticular formation itself and in the neighboring parvicellular reticular formation, which when combined may represent a significant terminal field for the PVH given the large rostrocaudal extent of axonal labeling here. Scattered axons were also found in the spinal trigeminal nucleus, primarily in lamina I and the paratrigeminal nucleus (Figs. 4I & 11 B-D). No axonal labeling was present in the hypoglossal nucleus (Fig 4G-J).

At the level of the area postrema, the NTS was the most densely innervated site in brainstem (Figs. 4H& I), and further details of this projection pattern are described below. At the level where the NTS borders the 4$^{th}$ ventricle (not shown), PVH axons formed close contacts with many C2 adrenergic neurons (Fig. 1 I in Supplemental Material). Also, a considerable amount of axonal labeling was present in the dorsomedial NTS subnucleus, with lesser amounts of axonal labeling in the gelatinous and parvicellular subnuclei. In the rostral NTS, the lateral and central subnuclei (Figs. 4F & G), which receive gustatory information from the tongue and oropharynx, contained very little axonal labeling.

The PVH projection was densest in regions of the medial and commissural subnuclei of the NTS, which receive input from gastrointestinal branches of the vagus nerve (Norgren and Smith, 1988). The density of axonal labeling was substantially reduced in the lateral subdivision of the NTS (Herbert et al., 1990), which includes the interstitial and ventrolateral subnuclei (Figs. 4H-J). In the medial NTS, a thicket of varicose axons and boutons enveloped neurons in two functionally-identified NTS subpopulations (Fig. 11): the A2 noradrenergic neurons and the aldosterone-sensitive neurons, which express 11-β-hydroxysteroid dehydrogenase type 2 (HSD2, green in Figure 16A; Geerling et al., 2006a; Geerling et al., 2006b). Dorsal to these two neuronal groups, a reduced density of axonal labeling was found in the medial NTS and in the dorsal part of the commissural nucleus, two sites which receive inputs from arterial baroreceptors (Ciriello, 1983; Housley et al., 1987). Likewise, there was a paucity of fibers in the dorsolateral part of the NTS, also a major termination site for baroreceptor afferents (Ciriello, 1983; Housley et al., 1987).

Whereas labeled axons in the medial and commissural NTS ramified extensively, fibers in the adjacent subpostremal NTS (and extending somewhat into the area postrema) were oriented in a rostrocaudal direction and formed many boutons *en passant* with minimal branching, viewed end-on in the coronal plane. Ventral to the medial NTS, the dorsal vagal nucleus exhibited moderately strong axonal labeling, but less than that found in the overlying NTS. The density of axonal labeling in the dorsal vagal nucleus increased at more caudal levels (cf. Fig. 4H with Figs. 4I & J). At first glance in sections that were not labeled for cell-type specific markers, a dense axon terminal field appeared to target a dorsolateral region of the dorsal vagal nucleus rostrally (Fig. 4H), but this labeling was actually concentrated in an area containing a rostral group of A2 noradrenergic neurons (Fig. 11C).

### PVH axonal labeling in association with central catecholamine neurons

Virtually every region of the brainstem that received input from the PVH also contained one or more groups of catecholamine neurons (see Supplemental Figure). Conversely, PVH axonal labeling was found within or near nearly every group of dopaminergic, noradrenergic, and adrenergic neurons (all labeled with tyrosine hydroxylase, TH). In some regions, catecholamine cells appear to be a primary target of axons from the PVH due to their co-extensive distribution with and apparent appositions from PHAL-labeled boutons (A1, A2, A10dc adrenergic and C1, C2, C3 adrenergic neurons). In other areas, catecholamine neurons are merely situated near many fibers of passage with minimal apparent varicosities (substantia nigra pars compacta/A9 dopaminergic and A7, A8 noradrenergic neurons) or lie at the periphery of a major terminal field targeting a separate group of neurons (the locus coeruleus/A6 and A4 noradrenergic neurons neighboring the

pre-LC; the A5 noradrenergic neurons adjacent to the lacrimal SSN; and the C2d neurons in the NTS, located dorsal to the A2 noradrenergic neurons).

## Discussion

The PVH projections to the brainstem are summarized in schematic form in Figure 12. These data are based on injections that involved both the PVH-dp and PVH-mp; no information was available regarding the descending projections that originate from the PVH-lp or PVH-f. Table 1 compares our results with data from other published studies. Several of the major findings are highlighted briefly here.

First, the medial NTS subnucleus at the level of area postrema along with its caudal continuation as the commissural nucleus receive the densest PVH input of the entire brainstem, and this labeling was especially concentrated in its ventral half, where the NTS abuts onto the underlying dorsal vagal nucleus. The PVH also provides a strong input to the dorsal motor nucleus of the vagus (DMX) – the site of origin for parasympathetic preganglionic neurons that project to the stomach (Shapiro and Miselis, 1985) and other gastrointestinal organs.

Second, the PVH projects densely to the pre-LC nucleus (and not to the LC as previously thought) and also forms close appositions on the HSD2 neurons of the NTS. Both of these brainstem sites have been implicated in salt appetite, suggesting that the PVH modulates ascending information pertaining to peripheral sodium status that is transmitted to higher brain levels (Geerling and Loewy, 2008).

Third, the PVH provides a strong input to a region of the superior salivatory nucleus (SSN), which gives rise to parasympathetic outflow to the cerebral and eye vasculature as well as to the glands of the eye, nasal cavity, and palate. One component of the PVH→SSN channel may serve a protective function by maintaining the cerebral and retinal blood flow within normal limits, especially during extreme physiological states, such as hypovolemia (see below). Separate PVH→SSN channels may safeguard both the corneal and nasopalatine mucosae from dehydration

Fourth, the heavy PVH projection to the caudal pressor area (CPA) may serve as part of a powerful descending sympathetic pathway that, until this report, has escaped attention and may be a major neural linkage for blood pressure regulation. Since the density of PVH axonal labeling in the CPA is considerably greater than what is seen in other sympathetic-related medullary sites, such as the RVLM and A5 region, it is likely that the PVH exerts a stronger influence through the CPA than it does on these two bulbospinal systems.

### Midbrain

The PVH projects only to a limited number of areas in the midbrain, and most of these areas received only a very light input. These areas include the ventral tegmental area (VTA), Edinger-Westphal nucleus (EW), ventrolateral periaqueductal gray matter (PAGvl), midbrain reticular formation (MRF), and dorsal raphe nucleus.

The PVH projection to the VTA is sparse (Fig 4A), and it is uncertain whether the PVH axons that branch in this region contact dopaminergic neurons, local interneurons, or both. Similarly, the EW region receives a sparse input from the PVH (Fig. 4A), considerably less than suggested in previous reports (Luiten et al., 1985;Zheng et al., 1995). There are two separate subpopulations of EW neurons: cholinergic parasympathetic neurons and centrally-projecting urocortin neurons, and neither group receive more than a few possible appositions.

A moderately dense axon terminal field was distributed in the PAGvl. It is impossible for us to state with certainty that this projection arises entirely (or at all) from neurons within PVH, or from neurons lying dorsolateral to the PVH in a region that as been termed the incerto-hypothalamic area, which is located in the vicinity of the A13 group of dopaminergic neurons (Sita et al., 2007).

Previous anterograde tracing studies showed extensive labeling in the lateral and dorsolateral PAG produced by PHAL injections that involved much of the dorsal PVH, which likely extended well beyond its borders, although only minimal details of the injection sites were provided (Luiten et al., 1985; Zheng et al., 1995). In our experiments, these PAG regions were labeled only when an injection involved the A13 group or incerto-hypothalamic zone, consistent with published anterograde tracing data (Sita et al., 2007). Our inference that most projections to the dorsolateral and lateral PAG originate outside the PVH is also consistent with the limited retrograde tracing data that is available regarding PAG afferents (Beitz, 1982). A re-examination of this issue is needed, particularly with the use of restricted retrograde tracer injections into the various subdivisions of the PAG. Thus, if PVH projects to the PAG, it targets the ventrolateral subdivision.

The PVH axonal labeling in the MRF exhibited a moderate number of varicosities intermixed with many fibers of passage. The MRF has been implicated in the patterning of motor behaviors, and may coordinate locomotor behavior through its descending linkage to the bulbospinal neurons which project to the spinal cord and modulates the somatomotor outflow; this MRF area is sometimes referred to as the midbrain locomotor region (Hathout and Bhidayasiri, 2005). Also, retrograde tracing data confirm that the PVH is a minor source of afferents to one of the cholinergic nuclei embedded in this region – the pedunculopontine nucleus, which has been implicated in extrapyramidal motor control and arousal (Steininger et al., 1992). Thus, PVH axons that target this region could influence locomotor behavior, generalized motor tone, and/or arousal. PVH projections to the MRF and pedunculopontine nucleus may be responsible for the alerting and orienting movements of the head and neck that occur when the PVH is stimulated in awake, behaving animals (Kannan et al., 1989).

The PVH projects to the dorsal raphe nucleus, and supplies a moderately dense terminal field that was primarily associated with neurons in the A10dc dopaminergic group (Fig. 4B). These cells have been implicated in the maintenance of wakefulness (Lu et al., 2006a), and provide much of the dopaminergic input to nuclei in the central extended amygdala complex (Hasue and Shammah-Lagnado, 2002;Shin et al., 2008). The functional role of this projection is unknown.

### Parabrachial nucleus

The PVH selectively targets the PB subnuclei that receive viscerosensory information from the medial NTS (Herbert et al., 1990), including primarily the external lateral PBel), caudal lateral (PBcl), and dorsal lateral PB (PBdl) subnuclei (Moga et al., 1990). PVH axons also ramify within a small, dorsomedial sector of the medial PB (PBm) in continuity with labeling in the pre-LC (Moga et al., 1990), a pattern nearly identical to that produced by PHAL injections into the aldosterone-sensitive subregion of the medial NTS at the level of the area postrema (see Fig. 2C of Geerling and Loewy, 2006b). Labeled axons were also found in the waist area of the PB (Moga et al., 1990) (see our Figs.4D & 5D).

In contrast, very little labeling was found in thermosensory and nociceptive parts of the PB, which are located rostral and lateral to its NTS-innervated subregions and receive input from the spinal cord (Cechetto et al., 1985; Hermanson and Blomqvist, 1996; Nakamura and Morrison, 2008). Likewise, minimal labeling was found in caudal parts of the medial PB

which receive gustatory input from the rostral NTS (Herbert et al., 1990) or in the rostral-medial region implicated in REM sleep control (Lu et al., 2006b).

Many neurons in the lateral PB subnuclei targeted by the PVH are activated in response to changes in osmolarity, extracellular fluid volume, immune activation, and gastrointestinal stimuli (Mayne et al., 1998; Richard et al., 2005; Geerling and Loewy, 2007b). Perhaps, the input from the PVH adds to the stimulatory input of their primary afferents in the NTS. For example, PVH neurons are activated by sodium-sensitive, osmosensitive, and angiotensin II (hypotension)-sensitive neurons in the subfornical organ (SFO) and organum vasculosum of the lamina terminalis (OVLT) – the forebrain circumventricular organs, which provide additional information about blood volume and tonicity. These and other signals from neurons located in the PVH and other forebrain sites that project to the lateral PB (lateral hypothalamic area, central nucleus of the amygdala -CeA, and bed nucleus of the stria terminalis -BST) likely modify the primary activity of its neurons, which is delivering viscerosensory information from the NTS to the forebrain. These modulatory projections add a layer of complexity and control to what is otherwise a straightforward pathway from the medulla to the forebrain.

Neurons in these PVH-innervated subnuclei of the lateral PB may play a critical role in relaying ingestive feedback information involving mechanical distention of the stomach (Karimnamazi et al., 2002), as well as its nutrient content (Yamamoto and Sawa, 2000) and noxious chemical information relayed from neurons in the area postrema. This feedback information is important for limiting ingestive behavior under normal conditions, and in more extreme states it produces nausea and conditioned taste aversions in response to perceived threats to the organism.

The PVH is the most sensitive site in the entire brain for increasing feeding behavior by microinjections of either adrenergic agonists (Leibowitz, 1978) or neuropeptide Y (NPY, Stanley and Leibowitz, 1985). Norepinephrine, epinephrine, and NPY all stimulate food intake in the PVH by acting on inhibitory G-protein-coupled receptors – the α-2-adrenergic and Y1/Y5R (Goldman et al., 1985; Kalra et al., 1991; Gerald et al., 1996). This PVH-inhibitory mechanism boosts food intake, even in satiated rats (Leibowitz, 1975), but feedback inhibition of ingestive behavior is still in operation, just at a reduced level. These findings suggest that PVH neurons provide a tonic input to some part(s) of the brain that inhibit ingestive behavior.

By augmenting the activity of viscerosensory pathways that mediate the feedback inhibition of food, water, and salt ingestion, the PVH projection to the lateral PB (and probably more so to the NTS, as discussed below) is a prime candidate for explaining its tonic inhibitory influence on ingestive behavior. Specifically, norepinephrine and NPY may inhibit neurons in the PVH, thus reducing the activity of neurons in the lateral PB, resulting in a reduction in the gain of appetite-inhibitory viscerosensory signals relayed to appetite-regulatory regions of the forebrain. This hypothesis is consistent with the finding that the PVH-mediated adrenergic feeding response can be eliminated by bilateral knife-cuts in the brainstem just rostral or caudal to the PB (McCabe et al., 1984), where descending fibers from the PVH course into the lateral PB and towards caudal medulla (see Fig. 4B-D). Through these descending projections to the lateral PB and medial NTS, the PVH may form one of the major nodal points for the control of food intake. Supporting this idea, PVH afferents arise in many appetite-regulatory nuclei which release endogenous inhibitory neurotransmitters, including A1 noradrenergic and C1 adrenergic neurons, which also express NPY (Sawchenko et al., 1985), GABAergic neurons in the arcuate hypothalamic nucleus that express NPY (Broberger et al., 1998; Broberger et al., 1999), and the loosely-organized ring

of GABAergic afferents that surround the PVH (Roland and Sawchenko, 1993; Boudaba et al., 1996).

### Pre-locus coeruleus

The pre-locus coeruleus (pre-LC) receives one of the densest PVH axon terminal fields in the entire brainstem, second only to the NTS. Thus, one of the most important findings presented here is that the overwhelming majority of PVH axons in this region target the pre-LC, not the LC.

In various research publications, it is not uncommon to see the LC defined as an overly-large subregion of the periventricular gray matter of the 4$^{th}$ ventricle. For example, one widely used rat brain atlas simply labels most of the territory along the medial aspect of the mesencephalic trigeminal nucleus as “LC” (Paxinos, 1998). Likewise, every previous PVH anterograde tracing study has either implied or explicitly concluded that the LC is its primary target in this region (Swanson, 1977; Luiten et al., 1985; Zheng et al., 1995; Toth et al., 1999).

The LC is a compact population of exclusively noradrenergic neurons, readily identifiable by their expression of catecholamine-synthetic enzymes. Their dendritic processes extend outside the core of this nucleus, primarily in a rostral and medial direction. As shown here in the coronal and sagittal planes (Fig. 5 and 6A), their cell bodies and perinuclear dendritic processes are largely excluded from the dense terminal field of axons from the PVH, which is centered rostral and ventral to the LC.

A major afferent projection from the PVH to the LC was proposed originally based on retrograde labeling after horseradish peroxidase (HRP) injections targeting the LC (Cedarbaum and Aghajanian, 1978). Later experiments, in which HRP injections were restricted to the core of the LC, suggested that a smaller number of neurons in the PVH-dp innervate the LC (Aston-Jones et al., 1986). In agreement with earlier data (Moga et al., 1990), only a few scattered PVH axons were seen in the LC core, although some appositions with TH-ir dendrites were found rostral and medial to the nuclear core of the LC. These findings are consistent with an electron microscopic study which found that even after restricting analysis to this peri-LC dendritic subregion, only a minority of synaptic terminals from the PVH (~20%) contact TH-containing structures (Reyes et al., 2005). Thus, even within this densely-packed region of noradrenergic dendrites surrounding the LC core, which overlap some of the axonal labeling at the periphery of the pre-LC terminal field, very few axons from the PVH innervate noradrenergic neurons in or around the LC.

Instead, the bulk of the PVH projection targets a group of neurons located just rostral to the LC: the pre-LC. This pattern – a dense axonal projection to the pre-LC coupled with an unexpectedly minor involvement of neurons in the LC – is similar to the ascending projections from the NTS (Van Bockstaele et al., 1999; Geerling and Loewy, 2006b) and to descending projections from the CeA (Van Bockstaele et al., 1996; Petrovich and Swanson, 1997) . It would not be surprising if future work revealed that additional afferents that were previously assumed to target the LC instead innervate the pre-LC.

The pre-LC, which appears to be more closely related to the PB than to the LC or other groups in the periventricular gray matter of the 4$^{th}$ ventricle – was discovered by neural tracing and c-Fos observations. Its neurons, which are partially intermixed with the caudal level of the mesencephalic nucleus of the trigeminal nerve, receive a dense projection from the aldosterone-sensitive HSD2 neurons in the NTS (Geerling and Loewy, 2006b), which are selectively activated by dietary sodium deprivation and other chronic volume-deficient conditions (Geerling et al., 2006a; Geerling and Loewy, 2007a). Correspondingly, in

response to dietary sodium deprivation, neurons in the pre-LC exhibit prominent c-Fos activation (along with a thin stripe of neurons along the inner edge of the PBel, which are likewise innervated by HSD2 neurons in the NTS; Geerling and Loewy, 2007b).

The present results identify the pre-LC as one of the most prominent recipients of axonal projections from the PVH. This discovery re-focuses questions about hypothalamic input to this region away from LC-related functions like behavioral arousal and cognition towards new possibilities related to the connections and functions of neurons in the pre-LC. In addition to the PVH and aldosterone-sensitive neurons in the NTS, the pre-LC appears to receive dense input from serotonergic neurons in the dorsal raphe (see Fig. 1a-c of Copray et al., 1991), and inhibitory neurons in the CeA and BST (Petrovich and Swanson, 1997; Dong et al., 2001) and probably a number of other sites (Geerling and Loewy, 2006b). Given the pronounced sodium deprivation-associated c-Fos activation of neurons in the pre-LC (Geerling and Loewy, 2007b), the projection shown here suggests that the PVH may contribute significantly to their activation during chronic sodium-deficient states. Neurons in the PVH are potently activated by the SFO and OVLT, forebrain circumventricular organs whose neurons are highly sensitive to changes in angiotensin II, a major endocrine signal for inadequate extracellular fluid volume and a major stimulus for sodium appetite (Geerling and Loewy, 2008). If neurons in the pre-LC are involved in mediating hedonic-appetitive responses to sodium deficiency, as we have hypothesized (Geerling and Loewy, 2007b; Geerling and Loewy, 2008), then the diversity of psychological, physiological, and pharmaceutical stimuli that stimulate neurons in the PVH may also modify salt-ingestive behavior under a variety of conditions that are not specifically related to sodium homeostasis, such as changes in affect, illness, or drug therapy.

In summary, neurons in the pre-LC integrate (1) ascending input from aldosterone-sensitive neurons in the NTS, which provide information specifically associated with systemic sodium deficiency, (2) descending input from the neurons in the PVH, which provide information more broadly associated with perturbations in volume status, osmolarity, and/or extracellular sodium concentration (in addition to a variety of other physical and psychological stressors), and (3) input from other sites in the brainstem and forebrain, including the BST, CeA, and dorsal raphe nucleus, all of which have been implicated in salt-ingestive behavior. These connections suggest that the pre-LC is uniquely positioned among brain sites involved in sodium homeostasis, and hence, these neurons may represent a critical neural link that mediates affective and appetitive responses that occur following perturbations in sodium balance.

### Superior salivatory nucleus

We found an intense PVH projection to the superior salivary nucleus (SSN). There, PVH axons target neurons primarily in a rostral, ventrolateral subregion, which is located just dorsolateral to the superior olivary and facial motor nuclei. The SSN contains a large population of cholinergic preganglionic neurons that send their axons out of the brainstem in the intermediate nerve (a part of the VII$^{th}$ cranial nerve) to innervate parasympathetic ganglia. Neurons distributed in more caudal and dorsolateral regions of the SSN regulate salivary function (submandibular and sublingual salivary glands, via the submandibular ganglion), whereas neurons in the more densely PVH-innervated subregion shown here form a small, compact group that primarily innervates cells in the pterygopalatine ganglion. These ganglion cells do not innervate the salivary glands but rather project to the lacrimal glands, nasopalatine mucosa, and the retinal and cerebral vasculature (Contreras et al., 1980; Nakai et al., 1993; Cuthbertson et al., 2003). Thus, concerning this latter subregion in particular, the term “salivatory nucleus” is really a misnomer, but it is widely used (Paxinos, 1998; Swanson, 1998), and we will follow this convention.

By contrast, the inferior salivatory nucleus (ISN) consists of parasympathetic preganglionic neurons along the rostral ventral edge of the nucleus of the solitary tract. Their axons join the glossopharyngeal ($IX^{th}$) nerve and terminate in the otic ganglion, which provides the parasympathetic innervation of the parotid gland. Some parasympathetic preganglionic neurons contributing to each of the $VII^{th}$ and $IX^{th}$ nerves tend to be located in positions between the two major cell groups, along the medial edge of the spinal trigeminal nucleus (Contreras et al., 1980). A small contingent of PVH axons were present in this region of the reticular formation, but no prominent relationship was seen here between PVH axons and ChAT-labeled neurons, in contrast to the dense terminal field found surrounding neurons in the rostral, ventrolateral SSN.

Retrograde transport studies have identified labeled neurons in the PVH after injections of tracer into this region of the caudal ventrolateral pons and rostral ventrolateral medulla (Byrum and Guyenet, 1987) – or after injecting a viral transneuronal tracer (pseudorabies virus) into the pterygopalatine ganglion (Spencer et al., 1990). Most of the earlier PVH anterograde tracing studies did not mention whether there was PVH axonal labeling in the SSN (Saper et al., 1976; Swanson, 1977; Gerfen and Sawchenko, 1985; Luiten et al., 1985). Zheng and colleagues identified a group of PHAL-labeled axons in the “A5 region” (Zheng et al., 1995), but did not compare this axonal labeling with a marker for catecholaminergic neurons, leaving this designation uncertain. They also illustrated a prominent cluster of axons in one of their figures (Fig. 2F of Zheng et al., 1995), which they identified as the “nucleus ambiguus,” but from its more rostral location and its position just dorsolateral to the facial motor nucleus, this was probably the SSN. The clearest previous description of PVH input to the SSN was provided by Hosoya and colleagues (1990), who demonstrated that axons from the PVH (and from the neighboring LHA; Hosoya et al., 1983) form a dense terminal field which is preferentially associated with neurons that extend their axons into the greater superficial petrosal nerve (i.e., the SSN), whereas the A5 noradrenergic neurons receive substantially less input. Our results confirm those findings.

Given that neurons in this part of the SSN influence parasympathetic functions unrelated to the production and release of saliva, what are the likely functional roles of this projection from the PVH? Two of the end-organ targets innervated by the pterygopalatine ganglion and therefore regulated by the SSN are the lacrimal glands and the mucosa of the nose and palate. In response to noxious stimuli, pterygopalatine parasympathetic fibers may reflexively stimulate lacrimation and mucous secretion in the nasal and oral cavities. As neurons in the SSN region receive direct excitatory input from the spinal trigeminal nucleus (McCulloch and Panneton, 1997; Panneton et al., 2000), noxious stimuli may increase lacrimal and nasopalatine secretions via a trigeminal-lacrimal reflex pathway.

Currently, there is no functional or even direct anatomical evidence that axons from the PVH in fact synapse directly on parasympathetic preganglionic neurons that regulate the lacrimal or nasopalatine mucous glands. Even in the absence of these data, it is worth considering that the trigeminal-lacrimal reflex pathway could be modulated by the PVH. For example, the activity of many neurons in the PVH is highly sensitive to immune activation (Elmquist and Saper, 1996; Li et al., 1996; Buller et al., 2003), suggesting that that the PVH may enhance (or directly activate) lacrimation and rhinorrhea – characteristic symptoms of upper respiratory infections and allergic rhinitis which are also influenced by other physiologic variables that increase PVH neuronal activity, including stress and circadian factors.

Another major end-organ target of this parasympathetic pathway is the cerebral vasculature. Neurally-mediated dilatation of cerebral vessels was first demonstrated in the early 1930s (Chorobski and Penfield, 1932; Cobb and Finesinger, 1932). Subsequent findings confirmed

that this pathway originates in the SSN (Nakai et al., 1993) and is controlled via a parasympathetic network of fibers that originates in the pterygopalatine ganglion. These ganglion cells produce acetylcholine, vasoactive intestinal polypeptide, and nitric oxide synthase (Hara et al., 1985; Okamura et al., 2002). Their axons run along the media and adventitia of large and medium-sized cerebral arteries, where their action potentials cause a calcium-dependent increase in the synthesis of nitric oxide, which dilates cerebral arteries by promoting the cGMP-dependant relaxation of vascular smooth muscle (Okamura et al., 2002).

The functional range of this vasodilatation is estimated at between 10 to 60% based on measurements of the maximum increase in vessel diameter and blood flow (Cobb and Finesinger, 1932; Okamura et al., 2002; Talman et al., 2007), yet no consensus has emerged regarding its homeostatic and/or pathophysiologic function(s). Neurons in the SSN have been implicated in the pathophysiologic vasodilatation that occurs during the breakdown of cerebral autoregulation with severe and acute increases in blood pressure (Agassandian et al., 2003). Thus, one possible role for the PVH projection to the SSN may be to produce cerebral vasodilatation in response to dehydration, hypovolemia, hemorrhage, and hypoglycemia, all of which activate neurons in the PVH. This raises the possibility that the PVH → SSN channel may produce adaptive changes in the so-called “autoregulation” of cerebral blood flow as occurs in response to extreme homeostatic challenges, such as profound volume depletion or hemorrhage.

### Ventral medullary surface

In every PVH-injected case, a large bundle of varicose axons coursed through the ventral medullary chemoreceptor zone, a superficial band that extends laterally from the pyramidal tracts along the ventral surface of the medulla. This region contains small neurons with dendritic processes that sometimes penetrate the superficial glia of the marginal layer (less than ~150 μm deep to the pial surface; Okada et al., 2001). This property may give them special access to the cerebrospinal fluid of the basilar cistern (due to their proximity to pial invaginations of the subarachnoid space in this region), and they may also have increased access to the blood plasma, due to the close relationship of some neurons with small branches of the basilar artery that penetrate the ventral medulla (Okada et al., 2001). Along this superficial region of the ventral medulla, many neurons are activated under conditions of hypercarbia, hypoxia, and other chemical stimuli (Sato et al., 1992; Berquin et al., 2000).

The retrotrapezoid nucleus (RTN) is subset of the chemosensitive neurons in the rostral part of the ventral medullary surface which lies ventral and immediately caudal to the facial nucleus (Rosin et al., 2006). In the earlier physiological literature, this region was referred to as the chemosensitive area “M”, and now, evidence has been collected that show these neurons are critical for the hyperventilatory response to hypercarbia (Guyenet, 2008). This region contains glutamatergic, non-monoaminergic neurons (Weston et al., 2004) that express the transcription factor Phox2b (Stornetta et al., 2006) and exhibit multisynaptic connections to the phrenic motoneurons (Dobbins and Feldman, 1994). These neurons are unusually sensitive to decreases in extracellular pH (Mulkey et al., 2004), which is the physiologic signature of hypercarbia, and a critical stimulus for breathing (Loeschcke, 1982). Destroying these neurons produces CO2-insensitivity and hypoventilation (Nattie and Li, 2002; Dubreuil et al., 2008; Takakura et al., 2008), which are the hallmarks of the congenital central hypoventilation syndrome (CCHS), a human disease associated with mutations in Phox2b (Weese-Mayer et al., 2005). In previous work, retrograde tracer injections into the RTN identified the PVH as a likely source of input (Rosin et al., 2006). Although we did not analyze the specific relationship between the aforementioned markers for pH-sensitive pre-respiratory neurons in the RTN and PVH axonal labeling in this study,

the present results support this conclusion by demonstrating that varicose axons from the PVH densely blanket the RTN (see Fig. 4F and Fig. 7).

This PVH→RTN projection may increase the gain of respiratory chemosensitivity in response to a wide variety of stressors that activate neurons in the PVH. Although presently untested, the PVH could be a site of origin for the so-called hypothalamic “command” signal that stimulates hyperpnea during physical exercise (Eldridge et al., 1981; Guyenet, 2008).

Apart from the RTN, additional $CO_2$ chemosensitive neurons populate the ventral medullary region. In the rat, these are distributed from the caudal edge of the facial nucleus to ~1.00 mm behind to the obex (Sato et al., 1992). Besides these neurons, dendrites originating from neurons of the ventral respiratory column also project into this zone. For example, some Bötzinger complex neurons have dendrites that extend to the ventral medullary surface (Pilowsky et al., 1990; Sun et al., 1994), some of which terminate in its glial border (Pilowsky et al., 1993). Furthermore, many non-respiratory neurons, such as the C1 adrenergic neurons, send dendrites into this region (Lipski et al., 1995). Since a large expanse of the ventral medullary surface is inundated with an extensive distribution of axons from the PVH, which travel in the rostrocaudal axis and form numerous *en passant* boutons, it is possible that the PVH influences a range of cardiorespiratory functions via these synaptic connections.

A small number of the serotonergic neurons in the parapyramidal region of the ventral medullary surface received appositions from PVH axons (data not shown). These serotonergic neurons are exclusively GABAergic and many are bulbospinal neurons, with direct projections to the intermediolateral cell column (Loewy and McKellar, 1981; Millhorn et al., 1987; Stornetta and Guyenet, 1999). However, most PVH axons coursing along the ventral surface did not contact any monoaminergic cell bodies (serotoninergic or catecholaminergic) or proximal dendrites. Instead, bulk of the PVH axons traveling along the ventral medullary surface were located just lateral to the parapyramidal region.

### Nucleus Ambiguus

Within the ambiguus complex, most axons from the PVH target the compact formation (NAc). Its cholinergic motoneurons innervate the esophagus and stimulate esophageal peristalsis, a critical component of swallowing. These densely-packed neurons display distinctive morphologic features, including longitudinal dendritic bundling and dendritic-somatic appositions (Hopkins, 1995).

Esophageal motoneurons in the NAc receive vagal afferent information from the esophagus via a relay in the central subnucleus of the NTS (Cunningham and Sawchenko, 1989), forming a short reflex loop that is interrupted by only one central interneuron (esophageal sensory neurons in the vagal nodose ganglion → NTScen → NAc → esophageal muscles). Despite a historical focus on this dense projection, which mediates a critical part of the swallowing reflex, ultrastructral analysis indicates that esophageal motoneurons in the NAc receive the majority of their synaptic input (~80%) from sources outside the NTS (Hayakawa et al., 1997). Based on the dense PVH→NAc projection identified here, the PVH represents an important source of input to these neurons, and may exert a major influence over esophageal motility.

Other NA subdivisions receive somewhat less input from the PVH. Parts of the semi-compact formation (NAsc), which contains pharyngeal motoneurons (Hopkins et al., 1996), received a modest input, suggesting that the PVH may influence voluntary or reflexive motor control of the upper airway and pharynx. The loose formation (NA-L), whose motoneurons innervate the laryngeal musculature (Hopkins et al., 1996), received a

relatively sparse input, suggesting that the PVH may not exert a strong influence over phonation or airway constriction, at least not at the level of the NA. A dense cluster of PVH axons was consistently found in the reticular formation immediately dorsal to the NAsc or NA-L (just caudal to the NAc), which may contain interneurons that influence the underlying ambiguus complex or innervate dendrites from NA neurons that project dorsally into the reticular formation (Pilowsky et al., 1990; Sun et al., 1994). While the PVH is multisynaptically linked to the motor supply of the larynx (Waldbaum et al., 2001), sufficient details regarding the second-order patterns of viral transneuronal labeling in this part of the medulla were not supplied so it is impossible to deduce the potential sites (s) of interneurons that innervate the NA-L neurons. Finally, it should be noted that the PVH projects directly to the paratrigeminal nucleus (Figs. 4I & 10C) – a medullary site receives primary afferent inputs from pharynx and larynx (Saxon and Hopkins, 2006), and thus, this is another site where the PVH may modulate laryngeal functions.

Finally, within and around the NA, many small and less-intensely-stained cholinergic neurons in the external formation of the NA (NAex) were contacted by boutons from the PVH. This projection is localized in a region of the NA where cardioinhibitory parasympathetic and bronchomotor parasympathetic preganglionic neurons have been localized, with the latter lying in a slightly rostral position (McAllen and Spyer, 1976; McAllen and Spyer, 1978). Our material did not permit us to determine whether there is a preferential input to either of these two NAex neuronal groups. The anterograde labeling shown here extends the previous finding that retrograde tracer injections targeted to functionally-identified cardioinhibitory subregions of the NAex label neurons in the PVH (Stuesse and Fish, 1984), and could explain why stimulating the PVH in awake, behaving animals elicits bradycardia despite proportional increases in blood pressure and sympathetic nerve activity (see Fig. 2 of Kannan et al., 1989).

In summary, PVH neurons innervate subregions of the NA complex in a non-uniform pattern. The primary NA subdivisions targeted by this projection are implicated in esophageal motility (NAc), bronchoconstriction (NAex), and bradycardia (NAex).

### Dorsal motor nucleus of the vagus

The PVH provides a moderately dense input to the DMX. This site is the origin for the parasympathetic outflow that targets the stomach and pancreas, and to a lesser degree other gastrointestinal organs including the liver, small intestine, and cecum (Hopkins et al., 1996), although some controversy exists with regard to the vagal motor innervation of the latter structures (Sugitani et al., 1991).

The DMX is viscerotopically organized as longitudinal columns, with each column corresponding to a branch of the abdominal vagus nerve (Fox and Powley, 1985; Powley et al., 1992). Gastric motoneurons localized in the DMX exhibit a unique morphological characteristic, namely they have dendrites that project dorsally into the medial NTS region (Shapiro and Miselis, 1985; Rinaman et al., 1989). This sensory-motor lattice may function as a unit during endocrine and visceromotor responses, such as various phases of digestion (Powley et al., 1992). Consistent with this hypothesis, microstimulation of the DMX causes the release of insulin and glucagon from the pancreas along with gastric acid secretion (Laughton and Powley, 1987). By extrapolation, incoming projections from the PVH may coordinate or boost the gain of these responses in both the NTS and DMX (Zhang et al., 1999).

### A1 & C1 catecholamine neurons

Perhaps our most salient observation regarding catecholamine neurons in the ventrolateral medulla (VLM) is that the rostral C1 group – and the rostral VLM (RVLM) in general – receives less input from the PVH than neurons located further caudally in the C1 and A1 groups. The RVLM has been studied extensively because its spinal-projecting neurons are necessary for maintaining basal sympathetic tone and mediate a variety of sympathetic cardiovascular responses, including the baroreflex (Ross et al., 1984; Guyenet, 2006). The projection from the PVH to the RVLM (including the rostral C1 neurons) may contribute to the pressor response that can be elicited by stimulation of the PVH (Yang and Coote, 1998). A number of investigators have focused on this moderately-dense PVH→RVLM connection to explore the idea that, beyond direct PVH projections to sympathetic preganglionic neurons (SPNs), this relayed output channel (PVH → RVLM → SPNs) plays a major role in sympathoexcitatory responses driven by the PVH (Yang and Coote, 1998; Pyner and Coote, 1999; Pyner and Coote, 2000; Stocker et al., 2004; Stocker et al., 2006).

Separate sets of retrograde tracing results have been interpreted either as evidence that more neurons in the PVH project to the spinal cord than the RVLM (Shafton et al., 1998) or the converse (Pyner and Coote, 2000). These conclusions are difficult to reconcile, due in part to the variable locations and diffusion of tracers from each injection site, and due to the depiction in each study of just one rostrocaudal section (or none at all, Shafton et al., 1998) to represent an entire series of injection sites. Also, injections involving the dense white matter tracts in and around the RVLM probably produce a significant degree of false-positive labeling due to uptake by fibers of passage (Chen and Aston-Jones, 1995), including PVH axons traveling through the RVLM to reach the caudal medulla and spinal cord. Even so, tracer injections into the rostral-pressor region of the RVLM (including the rostral C1 group) produce far less retrograde labeling in the PVH than injections placed caudally, closer to the C1/A1 transition zone (Andrezik et al., 1981; Van Bockstaele et al., 1989), and relative to injections that extend ventrally towards the medullary surface (see Figs. 2-3 of Stocker et al., 2006). These findings are consistent with the progressive rostral-to-caudal increase in the density of PVH axonal varicosities in the VLM, and with the dense axonal labeling we observed along the ventral medullary surface.

The ventral medullary surface contains, in the vicinity of PVH axons, the processes of some catecholaminergic neurons, some of which are probably derived from C1 pressor neurons, and future work is needed to determine the extent to which any of these processes receive input from the PVH. TH-ir processes in this region exhibited rare contacts with PHAL-labeled fibers in our material, although PVH fibers could target a greater number of processes from the non-C1 (non-adrenergic) pressor neurons in the RVLM (Guyenet, 2006). Regardless, the direct innervation of the RVLM by the PVH is rather limited when compared with the dense terminal fields we found in other parts of the VLM, including a much denser projection to a separate pressor area, the caudal pressor area (discussed below). These findings, and the extensive PVH projections to SPNs, argue against the idea that its direct projection to the RVLM is the major route by which the PVH activates the sympathetic nervous system.

Caudal to the retrofacial pressor region of the RVLM, a dense collection of varicose axons target adrenergic and noradrenergic neurons in the C1/A1 transition zone. Caudal C1 and A1 neurons here form a more compact column and exhibit prominent c-Fos activation in response to glucoprivation elicited by 2-deoxy-glucose (2DG; Ritter et al., 1998; 2DG; Dinh et al., 2006). C1 adrenergic neurons in this caudal region of the VLM co-express the appetite-enhancing neuropeptide Y (Sawchenko et al., 1985) and represent the major adrenergic afferents to the hypothalamus, particularly the PVH (Cunningham et al., 1990; Ritter et al., 2001). In the dorsal medulla, C3 and C2 adrenergic neurons are similarly

activated by glucoprivation (Ritter et al., 1998), express NPY (Sawchenko et al., 1985), receive dense input from the PVH, and provide the balance of the adrenergic input to the PVH (Cunningham et al., 1990).

Some of the glucoprivation-activated neurons in the caudal C1 group may form the subpopulation of long-latency, spinal-projecting neurons in the VLM which provide a functionally-selective input to SPNs that stimulate epinephrine (versus norepinephrine) release from the adrenal medulla (Morrison and Cao, 2000). If so, the present findings add another layer of control to this epinephrine-selective glucoregulatory pathway (PVH→C1/A1→SPNs→adrenal chromaffin cells that produce epinephrine, which stimulates glycogenolysis in the liver to raise blood sugar). Consistent with this hypothesis, increases in adrenal nerve activity and plasma epinephrine are the most prominent autonomic and neuroendocrine effects produced by stimulating or disinhibiting neurons within the PVH (Katafuchi et al., 1988; Martin et al., 1991).

The importance of C1/A1 glucosensitive neurons for both autonomic and behavioral responses to hypoglycemia is suggested by (1) the finding of Morrison and colleagues that the descending inputs to SPNs that selectively elicit epinephrine release from the adrenal gland originate from a subset of neurons in the VLM that are exquisitely responsive to glucoprivation, yet insensitive to baroreceptor feedback (Morrison and Cao, 2000), and (2) demonstrations by Ritter and coworkers that selective destruction of adrenergic and noradrenergic neurons that project to the PVH eliminates the feeding response to glucoprivation (Ritter et al., 2001; Dinh et al., 2006).

These catecholamine neurons also project heavily to the PVH subregion that contains CRH-expressing neurons, which control the hypothalamic-pituitary-adrenal axis (Cunningham et al., 1990). This projection is necessary for the increase in glucocorticoid production that occurs in response to insulin-induced hypoglycemia and glucoprivation with 2DG (Ritter et al., 2003; Dinh et al., 2006).

Collectively, these responses to hypoglycemia – autonomic (epinephrine release), neuroendocrine (glucocorticoid production), and behavioral (increased appetite for sugars) – are referred to as the counterregulatory response. The dense axonal projection from the PVH to the C1/A1 transition zone is well-positioned to increase the gain of each component of this coordinated response, potentially explaining the finding that lesions involving the PVH produce chronic intermittent hypoglycemia in cats (Barris and Ingram, 1936). Through this projection, stress-related activity of neurons in the PVH, by increasing the gain of the counterregulatory response, may exacerbate the neuroendocrine, autonomic, and appetitive changes that characterize the metabolic syndrome of hypertension, hyperglycemia (diabetes), and hyperphagia (obesity).

Caudal to the C1/A1 transition zone, PVH axons densely target the A1 noradrenergic neurons all the way back to the cervical spinal cord. Axonal labeling associated with the A1 neurons was consistently denser than with C1 neurons in the rostral pressor region of the RVLM, but similar in density to neurons in the C1/A1 transition zone.

A1 noradrenergic neurons are activated by a wide variety of physiologic stressors, including physical exercise (Ohiwa et al., 2006), pain (Pan et al., 1999), immune activation (Buller et al., 2003), hypoxemia (Smith et al., 1995), hypovolemia (Buller et al., 1999), and hypernatremia (Hochstenbach and Ciriello, 1995; Geerling and Loewy, 2007a). Viscerosensory and noxious afferents to the A1 neurons arrive directly from the NTS and spinal cord (Day and Sibbald, 1989; Pan et al., 1999). The present data suggest that their activity is strongly influenced by neurons in the PVH, contributing information related to an expanded set of physiologic and psychological stressors.

For example, information about extracellular sodium concentration, osmolarity, and fluid volume may be directed to A1 neurons in large part by their vagally-innervated afferents in the NTS and area postrema, but neurons in the PVH may add complementary information that they derive from their osmo-, Na-, and angiotensin II-sensitive afferent neurons in nearby circumventricular organs (SFO and OVLT). Thus, input from PVH may augment the responses of A1 neurons to hypernatremia and hypovolemia.

A1 neurons project directly to anxiety- and appetite-related sites localized in the forebrain, including the ventrolateral BST (Woulfe et al., 1990; Shin et al., 2008) and the CeA (Roder and Ciriello, 1993). They also provide a dense and selective input to neuroendocrine cells in the hypothalamus, specifically targeting magnocellular neurons in the PVH and SON that release the antidiuretic hormone, arginine vasopressin (AVP), into the posterior pituitary gland (Sawchenko and Swanson, 1982b; Cunningham and Sawchenko, 1988). This A1→PVH/SON connection is critical for AVP release in response to certain physiologic stressors, including hypovolemia and pain (Day and Sibbald, 1989; Yamashita et al., 1989; Smith et al., 1995; Dinh et al., 2006).

The PVH→A1 projection shown here is consistent with a previous report that axons immunoreactive for oxytocin (derived from a small subset of parvicellular neurons in the PVH) densely target the A1 region of the VLM (Buijs et al., 1990). Also, injecting oxytocin into this region of the VLM selectively increases the activity of magnocellular AVP neurons in the hypothalamus (Buijs et al., 1990). Thus, neurons in the PVH, which are themselves activated by a variety of stress-related inputs, may activate A1 noradrenergic neurons in the caudal VLM, which in turn contribute to a variety of stress-related responses in the forebrain, including AVP release from magnocellular neurons in the PVH.

### Ventral Respiratory Column

The ventral respiratory column (VRC) is a functionally defined area in the ventrolateral medullary reticular formation that contains a range of different types of respiratory neurons; these lie ventral to the nucleus ambiguus (Alheid and McCrimmon, 2008; Goodchild and Moon, 2009). The PVH has been reported to project to a specific part of the ventral respiratory column – the pre-Bötzinger complex (Kc et al., 2002; Mack et al., 2002; Mack et al., 2007), which contains propriobulbar neurons that interconnect other respiratory areas, including those that project to the phrenic motoneurons (Dobbins and Feldman, 1994). We did not find evidence that PVH projects to any of the perikarya lying in the ventral respiratory column (Fig. 7), but this, of course, does not exclude the possibility that the PVH influences respiration via connections with VRC neurons that have radiating dendrites that extend well beyond their nuclear borders (Pilowsky et al., 1990; Bryant et al., 1993; Sun et al., 1994).

### Nucleus Tractus Solitarii

The NTS is most densely innervated site in the brainstem. This massive projection was identified in all previous anterograde tracing studies (Saper et al., 1976; Luiten et al., 1985; Zheng et al., 1995; Toth et al., 1999).

Axons from the PVH do not indiscriminately target every subnucleus of the NTS. For example, regions of the NTS that are associated with taste (rostral central and lateral subnuclei), swallowing (central subnucleus), phonation (interstitial subnucleus) and respiration (ventrolateral subnucleus) contained little or no axonal labeling. Using the NTS nomenclature developed in Saper's laboratory (Herbert et al., 1990), PVH axons primarily target the medial, commissural, parvicellular, and dorsomedial NTS subnuclei. Less axonal labeling was found in the gelatinous and intermediate subnuclei. The subpostremal

subnucleus was unusual in that it exhibited fibers running in a rostrocaudal direction with minimal branching in the transverse plane, but many *en passant* boutons, similar to the labeling found along the ventral medullary surface. The ventral part of the medial NTS (Figs. 4H, I & J) was more heavily innervated than its dorsal counterpart. This region contains dendrites originating from gastric vagal motoneurons that extend dorsally beyond their cytoarchitectural border (Shapiro and Miselis, 1985; Rinaman et al., 1989).

These NTS regions receive profuse afferents from the abdominal vagus nerve, conveying information related to gastrointestinal functions (Norgren and Smith, 1988). The NTS provides both local and ascending projections. Some local projections target the DMX and may regulate the cephalic reflex phase of digestion (Zafra et al., 2006) and other later-stage digestive reflexes (Powley et al., 1992), while other NTS neurons project to the forebrain (largely via a relay in the parabrachial nucleus), providing feedback information that regulates ingestive behavior (Contreras and Stetson, 1981; Edwards and Ritter, 1982; South and Ritter, 1983).

The PVH may play a prominent role in regulating ingestive behavior, and its massive projection to the NTS is well-positioned to increase the gain of NTS responses to vagal feedback signals from the stomach, an arrangement that would effectively reduce ingestive behavior. Consistent with this idea, most neurons in the NTS that receive input from the PVH are highly responsive to gastric distention (Rogers and Hermann, 1985; Banks and Harris, 1987). In many of these neurons, the PVH produces excitatory responses that are greater than or equal to that produced by vagal stimulation (Banks and Harris, 1987).

This gain-control mechanism, if tonically active, could explain why lesions of the PVH more than double food intake and weight gain in rats (Leibowitz et al., 1981), and why localized microinjections of inhibitory monoamines or neuropeptides into the PVH cause a dramatic increase in feeding behavior. Microinjection mapping studies identified the PVH as the most sensitive site in the brain for the increase in feeding behavior produced by alpha-adrenergic agonists like norepinephrine or clonidine (Leibowitz, 1978) and by neuropeptide Y (NPY; Stanley and Leibowitz, 1985). Increased feeding can begin within seconds to minutes after injection of norepinephrine (Leibowitz, 1978), but the primary effect is an increase in meal size, not frequency (Ritter and Epstein, 1975; Leibowitz et al., 1993). All the receptors implicated in these feeding responses – the α2-adrenoreceptor for norepinephrine/epinephrine (Goldman et al., 1985), and the Y1 and Y5 receptors for NPY (Kalra et al., 1991; Gerald et al., 1996) – are coupled to inhibitory G-proteins ($G_{\alpha i}$), which reduce neuronal activity by inhibiting cAMP synthesis (Dohlman et al., 1991).

Collectively, these findings imply that the PVH tonically inhibits ingestive behavior. Based on the present data, we propose that this tonic inhibition occurs via its extensive projections to neurons in the NTS (and to their relay neurons in the lateral parabrachial nucleus), which transmit viscerosensory feedback information to regulate the quantities of food, water, and salt that are ingested (Contreras and Stetson, 1981; Edwards and Ritter, 1982; South and Ritter, 1983). Consistent with this idea, PVH-norepinephrine feeding responses are largely reduced after lesions of the vagus nerve (Sawchenko et al., 1981). It was originally suggested that the PVH increases food intake by stimulating parasympathetic outflow to the pancreas, causing the β-cells to release insulin, which circulates back to the brain and stimulates ingestive behavior (Sawchenko et al., 1981). This hypothesis is not mutually exclusive with the one presented here, although three findings argue against it. First, norepinephrine and other bioactive molecules that enhance food intake when injected into the PVH probably do not produce their responses by activating PVH neurons; instead they inhibit them via $G_{\alpha i}$-coupled receptors, as discussed above. Second, the rapid onset of ingestive behaviors after PVH injections of norepinephrine (Leibowitz, 1978) suggests that

it acts through rapid synaptic circuitry within the CNS, not a peripheral endocrine mechanism. Third, the hypothesis of insulin-mediated appetite stimulation predicts that damage to the PVH would *decrease* (or not change) ingestive behavior, however such lesions, which eliminate feeding responses to α2-adrenergic agonists (Leibowitz et al., 1983; Shor-Posner et al., 1988), instead produce a prominent and sustained *increase* in meal size (Leibowitz et al., 1981).

In addition to its role in food intake, the PVH may also influence ingestive behaviors associated with sodium deficiency. This hypothesis is based on our observation that the PVH projects to the aldosterone-sensitive HSD2 neurons of the NTS (Fig. 11) and also projects to the pre-LC nucleus (Figs. 5 & 6A) which is a major target of the HSD2 neurons (Geerling and Loewy, 2006b). Both sites become activated in response to sodium deprivation (Geerling and Loewy, 2007b). The PVH input to HSD2 neurons is a new finding, and the density of this projection suggests that excitatory neurons in the PVH may supply an important part of their synaptic input, possibly on par with the dense projection from inhibitory neurons in the CeA (Geerling and Loewy, 2006a). Thus, the present findings suggest that the PVH may exert influence over at least two brainstem cell groups that are selectively associated with aldosterone action and chronic sodium deficiency – the HSD2 neurons of the NTS and the pre-LC.

The A2 noradrenergic neurons receive a dense input from the PVH, which is consistent with previous light and electron microscopic findings that demonstrated nearly every TH-ir neuron in this region receives synaptic appositions from the PVH (Toth et al., 1999). Like the A1 noradrenergic neurons, the A2 neurons project to the PVH and SON (Cunningham and Sawchenko, 1988). They innervate the entire PVH, including the CRH neurons (Sawchenko and Swanson, 1982b; Cunningham and Sawchenko, 1988). Activation of A2 neurons may thereby produce slightly different autonomic and neuroendocrine responses, including more hypothalamo-pituitary-adrenal axis activation (Ericsson et al., 1994) relative to the A1 noradrenergic neurons, which in the PVH and SON project almost exclusively to vasopressin-containing magnocellular neurons (Sawchenko and Swanson, 1982b; Day and Sibbald, 1989).

Many neurons in the NTS receive direct synaptic input from the vagus nerve and mediate brainstem autonomic reflexes via direct projections to the VLM. In contrast, NTS neurons that project to the PVH – the overwhelming majority of which are A2 noradrenergic neurons (Sawchenko and Swanson, 1982b; Moore and Guyenet, 1983; Hermes et al., 2006; Gaykema et al., 2007) – receive very few synapses directly from the vagus and, in contrast to their efferent projections to the forebrain, exhibit relatively insignificant axonal projections to the caudal VLM when compared with other NTS neuronal groups (Bailey et al., 2006; Hermes et al., 2006). Instead, A2 neurons integrate locally pre-processed vagal information along with descending input from the PVH (and other brain sites) and, among their other output targets, they recursively activate neuroendocrine cells in the PVH and SON, including parvicellular CRH neurons and magnocellular oxytocin neurons. Blood levels of oxytocin are linearly related to a continuum of gastrointestinal feedback signals in response to food ingestion and other vagal stimuli, which increase progressively from satiety through nausea (Verbalis et al., 1986), and the A2→PVH/SON projection may be responsible for this oxytocin response to food intake (Onaka et al., 1995). A2 neurons also may contribute to the viscerosensory inhibition of food intake via their projections to the parvicellular PVH, the CeA, and an appetite-associated region of the ventrolateral BST (Terenzi and Ingram, 1995; Shin et al., 2008). The substantial PVH→A2 projection shown here may confer more flexibility in their visceral processing and output functions that what is currently understood.

Moderate PVH axonal labeling was also found in the dorsomedial and commissural NTS regions that receive input from the arterial baroreceptors (Ciriello, 1983; Housley et al., 1987). This labeling extended somewhat into the “C2d” group of neurotensin-adrenergic baroreceptive neurons in the dorsomedial NTS (Higgins et al., 1984) suggesting that excitatory projections from the PVH to both pressor and depressor regions of the brainstem could exert simultaneously opposing effects on cardiovascular function – sympathoexcitation via the RVLM, caudal pressor area (see below), and sympathetic preganglionic cell column, yet sympathoinhibition via augmentation of the baroreflex in the NTS (in addition to activating cardiac parasympathetic neurons in the NAex). Contradicting this hypothesis, most neurons in the NTS that receive synaptic input from the PVH do not exhibit any cardiac or respiratory modulation; the few that do exhibit primarily an inhibitory response to stimulation of the PVH (Banks and Harris, 1987). Some gastrointestinal sensory NTS neurons, which are clearly the main modulating function of the PVH→NTS projection, do influence cardiovascular function by a multisynaptic inhibition of sympathetic outflow to the splanchnic vasculature (Sartor and Verberne, 2002). Thus, while there is little evidence that the PVH→NTS projection directly influences baroreflex function, it may alter cardiovascular function indirectly through this visceral-sympathoinhibitory interaction.

### Caudal Pressor Area

A poorly-understood region of the caudalmost ventrolateral medulla known as the caudal pressor area (CPA) receives an extremely dense input from the PVH. This region was not mentioned in previous PVH tracing studies (Saper et al., 1976; Swanson, 1977; Luiten et al., 1985; Zheng et al., 1995; Toth et al., 1999). Our identification of this major PVH→CPA connection is, however, consistent with other evidence in the literature. The dense axonal labeling we found within the CPA may have been evident in one photomicrograph from a prior PHAL tracing study, although the level of the medulla from which it was taken was not provided and the target was misidentified as a lateral part of the lateral reticular nucleus (Figure 3B of Zheng et al., 1995). Also, an oxytocin-immunoreactive axon terminal field (derived from a small subset of parvicellular neurons in the PVH) extends beyond the A1 noradrenergic neurons in this region and into what appears to be the CPA (see Fig. 1 of Buijs et al., 1990). Finally, retrograde tracer injections in this region of the caudal ventrolateral medulla produce extensive retrograde labeling in the PVH (Cobos et al., 2003).

The CPA is a complex region in the caudal medulla (Goodchild and Moon, 2009). Using microinjections of L-glutamate, the CPA was first localized in the rat brainstem by Gordon and McCann (1988) and later, a more precise location was identified by Sun and Panneton (2002). The CPA is defined functionally as the territory at the caudal extreme of the ventrolateral medulla in which exogenous chemical stimulation produces a large increase in blood pressure. The effective pressor region coincides with the pyramidal decussation and borders the caudal end of the lateral reticular nucleus on its medial side, the spinal trigeminal nucleus on its dorsolateral side, and white matter tracts ventrally. The most sensitive zone in this area is centered just lateral to the caudal A1 neurons (Sun and Panneton, 2002), indicating that its pressor neurons are distinct from catecholaminergic neurons in the ventral medulla. This region of the ventrolateral medulla contains a subpopulation of peptidergic (substance P/preprotachykinin-A-expressing) neurons (Li et al., 2005), and other, as-yet uncharacterized subpopulations of glutamatergic and GABAergic neurons (Seyedabadi et al., 2006).

Some disagreement exists regarding the specific mechanisms by which the CPA influences blood pressure, such as the (multi-)synaptic pathways by which its neurons influence the RVLM or the SPNs and the extent to which the activity of RVLM pressor neurons, or sympathetic tone in general, depend upon tonic input from neurons in the CPA (Gordon and McCann, 1988; Campos Junior et al., 1994; Possas et al., 1994; Campos and McAllen, 1999;

Natarajan and Morrison, 2000; Horiuchi and Dampney, 2002; Seyedabadi et al., 2006). Many seemingly inconsistent findings in previous studies could reflect the slightly different rostrocaudal locations of their injection and stimulation sites designated as “CPA”. Caudally, the CPA is continuous with a group of propriospinal neurons that lie in the lateral spinal nucleus and the dorsolateral funiculus, and these neurons project directly to the SPNs (Jansen and Loewy, 1997). This may explain why pressor responses elicited from the CPA are dependent upon the RVLM (Gordon and McCann, 1988; Possas et al., 1994; Natarajan and Morrison, 2000; Horiuchi and Dampney, 2002), while responses elicited from a caudal extension of this region, which extends caudally from the CPA to the C3 spinal level (termed the medullo-cervical pressor area, or MCPA) survive the pharmacologic inhibition of the RVLM and brainstem transection caudal to it (Seyedabadi et al., 2006). As shown here, varicose axons from the PVH target the entire rostral-caudal expanse of the CPA, and then extend caudally into the cervical spinal cord, where they may target rostral regions of the lateral spinal nucleus and dorsolateral funiculus designated functionally as the MCPA (Seyedabadi et al., 2006). Determining the extent to which the scattered pre-motor neurons of the lateral spinal nucleus and dorsolateral funiculus (Jansen and Loewy, 1997) and in the caudal end of the CPA (Seyedabadi et al., 2006; Iigaya et al., 2007) receive synaptic input from the PVH will be necessary to advance our understanding of the descending control of the sympathetic nervous system by the forebrain.

Some neurons in this general region of the caudal ventrolateral medulla receive nociceptive input from the spinal cord and medullary dorsal horn and exhibit c-Fos expression in response to noxious spinal or trigeminal stimuli (Craig, 1995; McCulloch and Panneton, 1997; Lima et al., 2002). This nociceptive population includes many A1 noradrenergic neurons (Pan et al., 1999), but it is unknown whether any nociceptive afferents target the CPA neurons that increase blood pressure.

CPA neurons project rostrally, targeting a subregion of the caudal ventrolateral medulla (CVLM) and a variety of other brainstem sites, including the region containing A5 and SSN neurons, a small nociceptive nucleus in the parabrachial complex (internal lateral PB subnucleus), the Kölliker-Fuse nucleus, and the caudal commissural NTS (Sun and Panneton, 2005). Based on its overall pattern of efferent projections from this region, it has been suggested that neurons in this region mediate pressor and possibly other responses to pain (Sun and Panneton, 2005). The CPA→CVLM projection probably mediates its pressor influence in the RVLM (Natarajan and Morrison, 2000), but the overall projection pattern of neurons in this region suggests that the CPA might do more than simply increase blood pressure. It is also located in the vicinity of the nucleus retroambiguus, a group of premotor neurons that directly innervate spinal motor neurons which control respiration and vocalization. The activity of neurons in the nucleus retroambiguus is largely governed by their input from the lateral PAG, which coordinates emotional motor behaviors and changes in autonomic function (Subramanian et al., 2008). The specific identity of CPA pressor neurons remains unknown, so it remains unclear whether they are targeted by the lateral PAG, but their location suggests that they could receive input in parallel with the nucleus retroambiguus, and may contribute to an autonomic component (sympathoexcitation) of lateral PAG-mediated emotional responses.

Based on what has been mentioned above, it is reasonable to hypothesize that the CPA serves as major link for the sympathoexcitatory-pressor responses that are elicited by activation of the PVH, perhaps stronger than the PVH→RVLM connection. Obviously, the PVH projection to the SPNs is the most direct route whereby the PVH can produce sympathoexcitation, but the present findings identify the CPA as a key relay site, which may provide the PVH one of its most potent linkages in the central control of the sympathetic nervous system.

### Conclusions

A number of new findings regarding the PVH projections to the brainstem were presented in this report. As a result of these anatomical observations, several novel hypotheses regarding the function of the PVH have been suggested.

Combined with functional data reviewed above, the present anatomical findings suggest that the PVH exerts a major influence over several physiological and behavioral functions. These include: the inhibitory control of food intake (via major projections to viscerosensory feedback neurons in the NTS and lateral PB), appetitive responses to sodium deficiency (via the aldosterone-sensitive HSD2 neurons in the NTS and their relay neurons in the pre-LC), changes in gastric and pancreatic functions (via the NTS and dorsal vagal nucleus), esophageal motor control (via the compact formation of the nucleus ambiguus), the counterregulatory response to hypoglycemia (via catecholamine neurons in the C1/A1 transition zone), hyperventilation (via the retrotrapezoid nucleus), protection of the cornea (lacrimation), nasal passages and oral cavity (serous and mucous secretions) as well as a potential neural safeguard for the vasculature of the brain and eye (via the superior salivatory nucleus), and several opposing mechanisms of cardiovascular control – sympathoexcitation (via the caudal pressor area and the C1 adrenergic neurons), vasopressin release (through A1 noradrenergic neurons), sympathoinhibition (via the NTS), and parasympathetic bradycardia (via the external formation of the nucleus ambiguus).

## Supplementary Material

Refer to Web version on PubMed Central for supplementary material.

## Acknowledgments

We thank Xay Van Nguyen for his excellent technical assistance, and Dennis Oakley for help with the confocal microscopy. Special thanks go to Drs. Jack L. Feldman, Patrice G. Guyenet, Paul A. Gray, David A. Hopkins, W. Michael Panneton, Paul Pilowsky, and Clifford B. Saper for useful discussions.

Grant sponsor:

National Heart, Lung, and Blood Institute of the National Institutes of Health - Grant number: HL025449, Bakewell Imaging Center Fund, and National Institutes of Health - Grant number: NS057105 Neuroscience Blueprint Core Grant.

## Abbreviations Used in Figures and Figure Legends

| | |
|---|---|
| **3V** | Third ventricle |
| **4V** | Fourth ventricle |
| **A1** | A1 noradrenergic cell group |
| **A2** | A2 noradrenergic cell group |
| **A2r** | A2 neurons, rostral cluster (along the dorsolateral border of DMX) |
| **A5** | A5 noradrenergic cell group |
| **A7** | A7 noradrenergic cell group |
| **A8** | A8 dopaminergic cell group |
| **A10dc** | Dorsal-caudal A10 dopaminergic neurons in dorsal raphe nucleus |
| **AHN** | Anterior hypothalamic nucleus |

| | |
|---|---|
| **AP** | Area postrema |
| **Aq** | Cerebral aqueduct |
| **Arc** | Arcuate hypothalamic nucleus |
| **Bar** | Barrington's nucleus (pontine micturition center) |
| **BötC** | Bötzinger complex of ventral respiratory column |
| **C1** | C1 adrenergic cell group |
| **C2** | C2 adrenergic cell group in the NTS |
| **C2d** | C2 adrenergic cell group in the dorsomedial NTS |
| **C3** | C3 adrenergic cell group in rostral dorsomedial medulla |
| **ChAT** | Choline acetyltransferase |
| **cp** | Cerebral peduncle |
| **CTb** | Cholera toxin beta-subunit |
| **CPA** | Caudal pressor area |
| **CU** | Cuneate nucleus |
| **CVLM** | Caudal ventrolateral medulla |
| **cVRG** | Caudal ventral respiratory group |
| **dscp** | Decussation of the superior cerebellar peduncles |
| **DMH** | Dorsomedial hypothalamic nucleus |
| **DMX** | Dorsal motor nucleus of the vagus |
| **DR** | Dorsal raphe nucleus |
| **DTN** | Dorsal tegmental nucleus |
| **EW** | Edinger-Westphal nucleus |
| **fr** | Fasciculus retroflexus |
| **fx** | Fornix |
| **GR** | Gracile nucleus |
| **HSD2** | 11-β-hydroxysteroid dehydrogenase type 2 (marker for aldosterone-sensitive neurons |
| **IC** | Inferior colliculus |
| **icp** | Inferior cerebellar peduncle |
| **III** | Oculomotor nucleus |
| **IRt** | Intermediate reticular nucleus |
| **IV** | Trochlear nucleus |
| **KF** | Kölliker-Fuse nucleus |
| **LC** | Locus coeruleus |
| **LDT** | Laterodorsal tegmental nucleus |
| **LHA** | Lateral hypothalamic area |

| | |
|---|---|
| **LRN** | Lateral reticular nucleus |
| **LSO** | Lateral superior olive |
| **MeV** | Mesencephalic nucleus of the trigeminal nerve |
| **ml** | Medial lemniscus |
| **mlf** | Medial longitudinal fasciculus |
| **MoV** | Motor nucleus of the trigeminal nerve |
| **MV** | Medial vestibular nucleus |
| **NA** | Nucleus ambiguus |
| **NAc** | Compact formation (esophageal motoneurons) |
| **NAex** | External formation (parasympathetic preganglionic neurons) |
| **NA-L** | Loose formation (laryngeal motoneurons) |
| **NAsc** | Semi-compact formation (pharyngeal motoneurons) |
| **NTS** | Nucleus of the solitary tract |
| **NTScom** | Commissural subnucleus of the NTS |
| **ot** | Optic tract |
| **PAG** | Periaqueductal gray matter |
| **PAGdl** | Dorsolateral subdivision of the PAG |
| **PAGvl** | Ventrolateral subdivision of the PAG |
| **PAT** | Paratrigeminal nucleus |
| **peri-LCrm** | Rostromedial dendritic extensions from the LC core |
| **PB** | Parabrachial nucleus |
| **PBcl** | Central lateral PB subnucleus |
| **PBdl** | Dorsal lateral PB subnucleus |
| **PBel** | External lateral PB subnucleus |
| **PBm** | Medial PB subnucleus |
| **PBwa** | Waist area of PB |
| **PHAL** | *Phaseolus vulgaris* leucoagglutinin |
| **PNMT** | Phenylethanolamine-N-methyltransferase |
| **PSV** | Principal sensory nucleus of the trigeminal nerve |
| **pre-BötC** | Pre-Bötzinger complex of ventral respiratory column |
| **pre-LC** | Pre-locus coeruleus nucleus |
| **PVH** | Paraventicular hypothalamic nucleus |
| **PVH-ap** | Anterior parvicellular PVH subdivision |
| **PVH-dp** | Dorsal parvicellular PVH subdivision |
| **PVH-f** | Forniceal PVH subdivision |
| **PVH-lp** | Lateral parvocellular PVH subdivision |

| | |
|---|---|
| **PVH-M** | Magnocellular PVH neurons |
| **PVH-mp** | Medial parvocellular PVH subdivision |
| **py** | Pyramidal tract |
| **RAmb** | Retroambiguus nucleus |
| **RM** | Raphe magnus nucleus |
| **RN** | Red nucleus |
| **RPA** | Raphe pallidus nucleus |
| **RO** | Raphe obscurus |
| **RRF** | Retrorubral field |
| **RTN** | Retrotrapezoid nucleus |
| **rVRG** | Rostral ventral respiratory group |
| **SC** | Superior colliculus |
| **scp** | Superior cerebellar peduncle (brachium conjunctivum) |
| **sctv** | Ventral spino-cerebellar tract |
| **SNc** | Substantia nigra, pars compacta |
| **SNr** | Substantia nigra, pars reticulata |
| **SON** | Supraoptic hypothalamic nucleus |
| **SpV** | Spinal sensory nucleus of the trigeminal nerve |
| **SPIV** | Spinal vestibular nucleus |
| **SptV** | Spinal tract of the trigeminal nerve |
| **SSN** | Superior salivatory nucleus |
| **SUV** | Superior vestibular nucleus |
| **t** | Solitary tract |
| **TH** | Tyrosine hydroxylase |
| **TRN** | Tegmental reticular nucleus |
| **VII** | Facial (VIIth nerve) nucleus |
| **VIIn** | VIIth cranial nerve (intracranial, post-genu) |
| **gVII** | Genu of the VIIth cranial nerve (dorsal, intracranial) |
| **VLM** | Ventrolateral medulla |
| **VMH** | Ventromedial hypothalamic nucleus |
| **VTA** | Ventral tegmental area |
| **XII** | Hypoglossal nucleus |
| **ZI** | Zona incerta |

## Literature Cited


Agassandian K, Fazan VP, Margaryan N, Dragon DN, Riley J, Talman WT. A novel central pathway links arterial baroreceptors and pontine parasympathetic neurons in cerebrovascular control. Cell Mol Neurobiol. 2003; 23:463–478. [PubMed: 14514008]

Alheid GF, McCrimmon DR. The chemical neuroanatomy of breathing. Respir Physiol Neurobiol. 2008; 164:3–11. [PubMed: 18706532]

Andrezik JA, Chan-Palay V, Palay SL. The nucleus paragigantocellularis lateralis in the rat. Demonstration of afferents by the retrograde transport of horseradish peroxidase. Anat Embryol (Berl). 1981; 161:373–390. [PubMed: 7247035]

Aston-Jones G, Ennis M, Pieribone VA, Nickell WT, Shipley MT. The brain nucleus locus coeruleus: restricted afferent control of a broad efferent network. Science. 1986; 234:734–737. [PubMed: 3775363]

Bailey TW, Hermes SM, Andresen MC, Aicher SA. Cranial visceral afferent pathways through the nucleus of the solitary tract to caudal ventrolateral medulla or paraventricular hypothalamus: target-specific synaptic reliability and convergence patterns. J Neurosci. 2006; 26:11893–11902. [PubMed: 17108163]

Banks D, Harris MC. Activation within dorsal medullary nuclei following stimulation in the hypothalamic paraventricular nucleus in rats. Pflugers Arch. 1987; 408:619–627. [PubMed: 3601646]

Barris RW, Ingram WR. The effect of experimental hypothalamic lesions upon blood sugar. Am J Physiol. 1936; 114:555–561.

Beitz AJ. The organization of afferent projections to the midbrain periaqueductal gray of the rat. Neuroscience. 1982; 7:133–159. [PubMed: 7078723]

Berquin P, Bodineau L, Gros F, Larnicol N. Brainstem and hypothalamic areas involved in respiratory chemoreflexes: a Fos study in adult rats. Brain Res. 2000; 857:30–40. [PubMed: 10700550]

Blair ML, Piekut D, Want A, Olschowka JA. Role of the hypothalamic paraventricular nucleus in cardiovascular regulation. Clin Exp Pharmacol Physiol. 1996; 23:161–165. [PubMed: 8819646]

Boudaba C, Szabo K, Tasker JG. Physiological mapping of local inhibitory inputs to the hypothalamic paraventricular nucleus. J Neurosci. 1996; 16:7151–7160. [PubMed: 8929424]

Broberger C, Johansen J, Johansson C, Schalling M, Hokfelt T. The neuropeptide Y/agouti gene-related protein (AGRP) brain circuitry in normal, anorectic, and monosodium glutamate-treated mice. Proc Natl Acad Sci U S A. 1998; 95:15043–15048. [PubMed: 9844012]

Broberger C, Visser TJ, Kuhar MJ, Hokfelt T. Neuropeptide Y innervation and neuropeptide-Y-Y1-receptor-expressing neurons in the paraventricular hypothalamic nucleus of the mouse. Neuroendocrinology. 1999; 70:295–305. [PubMed: 10567855]

Bryant TH, Yoshida S, de Castro D, Lipski J. Expiratory neurons of the Botzinger Complex in the rat: a morphological study following intracellular labeling with biocytin. J Comp Neurol. 1993; 335:267–282. [PubMed: 8227518]

Buijs RM, Van der Beek EM, Renaud LP, Day TA, Jhamandas JH. Oxytocin localization and function in the A1 noradrenergic cell group: ultrastructural and electrophysiological studies. Neuroscience. 1990; 39:717–725. [PubMed: 2097524]

Buller KM, Dayas CV, Day TA. Descending pathways from the paraventricular nucleus contribute to the recruitment of brainstem nuclei following a systemic immune challenge. Neuroscience. 2003; 118:189–203. [PubMed: 12676149]

Buller KM, Smith DW, Day TA. Differential recruitment of hypothalamic neuroendocrine and ventrolateral medulla catecholamine cells by non-hypotensive and hypotensive hemorrhages. Brain Res. 1999; 834:42–54. [PubMed: 10407092]

Byrum CE, Guyenet PG. Afferent and efferent connections of the A5 noradrenergic cell group in the rat. J Comp Neurol. 1987; 261:529–542. [PubMed: 2440916]

Campos RR Junior, Possas OS, Cravo SL, Lopes OU, Guertzenstein PG. Putative pathways involved in cardiovascular responses evoked from the caudal pressor area. Braz J Med Biol Res. 1994; 27:2467–2479. [PubMed: 7640640]

Campos RR, McAllen RM. Tonic drive to sympathetic premotor neurons of rostral ventrolateral medulla from caudal pressor area neurons. Am J Physiol. 1999; 276:R1209–1213. [PubMed: 10198405]

Cechetto DF, Standaert DG, Saper CB. Spinal and trigeminal dorsal horn projections to the parabrachial nucleus in the rat. J Comp Neurol. 1985; 240:153–160. [PubMed: 3840498]

Cedarbaum JM, Aghajanian GK. Afferent projections to the rat locus coeruleus as determined by a retrograde tracing technique. J Comp Neurol. 1978; 178:1–16. [PubMed: 632368]

Chen S, Aston-Jones G. Evidence that cholera toxin B subunit (CTb) can be avidly taken up and transported by fibers of passage. Brain Res. 1995; 674:107–111. [PubMed: 7773677]

Chorobski J, Penfield W. Cerebral vasodilator nerves and their pathway from the medulla oblongata, with observations on their pial and intracerebral vascular plexus. Archives of Neurology and Psychiatry. 1932; 28:1257–1288.

Ciriello J. Brainstem projections of aortic baroreceptor afferent fibers in the rat. Neurosci Lett. 1983; 36:37–42. [PubMed: 6856201]

Cobb S, Finesinger JE. Cerebral Circulation XIX. The vagal pathway of the vasodilator impulses. Archives of Neurology and Psychiatry. 1932; 28:1243–1256.

Cobos A, Lima D, Almeida A, Tavares I. Brain afferents to the lateral caudal ventrolateral medulla: a retrograde and anterograde tracing study in the rat. Neuroscience. 2003; 120:485–498. [PubMed: 12890518]

Contreras RJ, Gomez MM, Norgren R. Central origins of cranial nerve parasympathetic neurons in the rat. J Comp Neurol. 1980; 190:373–394. [PubMed: 7381063]

Contreras RJ, Stetson PW. Changes in salt intake lesions of the area postrema and the nucleus of the solitary tract in rats. Brain Res. 1981; 211:355–366. [PubMed: 7237128]

Coote JH. A role for the paraventricular nucleus of the hypothalamus in the autonomic control of heart and kidney. Exp Physiol. 2005; 90:169–173. [PubMed: 15604110]

Copray JC, Liem RS, Ter Horst GJ, van Willigen JD. Origin, distribution and morphology of serotonergic afferents to the mesencephalic trigeminal nucleus of the rat. Neurosci Lett. 1991; 121:97–101. [PubMed: 2020396]

Cotton RG, McAdam W, Jennings I, Morgan FJ. A monoclonal antibody to aromatic amino acid hydroxylases. Identification of the epitope. Biochem J. 1988; 255:193–196. [PubMed: 2461704]

Craig AD. Distribution of brainstem projections from spinal lamina I neurons in the cat and the monkey. J Comp Neurol. 1995; 361:225–248. [PubMed: 8543660]

Cunningham ET Jr. Bohn MC, Sawchenko PE. Organization of adrenergic inputs to the paraventricular and supraoptic nuclei of the hypothalamus in the rat. J Comp Neurol. 1990; 292:651–667. [PubMed: 2324319]

Cunningham ET Jr. Sawchenko PE. Anatomical specificity of noradrenergic inputs to the paraventricular and supraoptic nuclei of the rat hypothalamus. J Comp Neurol. 1988; 274:60–76. [PubMed: 2458397]

Cunningham ET Jr. Sawchenko PE. A circumscribed projection from the nucleus of the solitary tract to the nucleus ambiguus in the rat: anatomical evidence for somatostatin-28-immunoreactive interneurons subserving reflex control of esophageal motility. J Neurosci. 1989; 9:1668–1682. [PubMed: 2470875]

Cuthbertson S, LeDoux MS, Jones S, Jones J, Zhou Q, Gong S, Ryan P, Reiner A. Localization of preganglionic neurons that innervate choroidal neurons of pterygopalatine ganglion. Invest Ophthalmol Vis Sci. 2003; 44:3713–3724. [PubMed: 12939284]

Day TA, Sibbald JR. A1 cell group mediates solitary nucleus excitation of supraoptic vasopressin cells. Am J Physiol. 1989; 257:R1020–1026. [PubMed: 2589528]

Dinh TT, Flynn FW, Ritter S. Hypotensive hypovolemia and hypoglycemia activate different hindbrain catecholamine neurons with projections to the hypothalamus. Am J Physiol Regul Integr Comp Physiol. 2006; 291:R870–879. [PubMed: 16675637]

Dobbins EG, Feldman JL. Brainstem network controlling descending drive to phrenic motoneurons in rat. J Comp Neurol. 1994; 347:64–86. [PubMed: 7798382]

Dohlman HG, Thorner J, Caron MG, Lefkowitz RJ. Model systems for the study of seven-transmembrane-segment receptors. Annu Rev Biochem. 1991; 60:653–688. [PubMed: 1652922]

Dong HW, Petrovich GD, Watts AG, Swanson LW. Basic organization of projections from the oval and fusiform nuclei of the bed nuclei of the stria terminalis in adult rat brain. J Comp Neurol. 2001; 436:430–455. [PubMed: 11447588]

Dubreuil V, Ramanantsoa N, Trochet D, Vaubourg V, Amiel J, Gallego J, Brunet JF, Goridis C. A human mutation in Phox2b causes lack of CO2 chemosensitivity, fatal central apnea, and specific loss of parafacial neurons. Proc Natl Acad Sci U S A. 2008; 105:1067–1072. [PubMed: 18198276]

Edwards GL, Ritter RC. Area postrema lesions increase drinking to angiotensin and extracellular dehydration. Physiol Behav. 1982; 29:943–947. [PubMed: 7156231]

Eldridge FL, Millhorn DE, Waldrop TG. Exercise hyperpnea and locomotion: parallel activation from the hypothalamus. Science. 1981; 211:844–846. [PubMed: 7466362]

Elmquist JK, Saper CB. Activation of neurons projecting to the paraventricular hypothalamic nucleus by intravenous lipopolysaccharide. J Comp Neurol. 1996; 374:315–331. [PubMed: 8906501]

Ericsson A, Kovacs KJ, Sawchenko PE. A functional anatomical analysis of central pathways subserving the effects of interleukin-1 on stress-related neuroendocrine neurons. J Neurosci. 1994; 14:897–913. [PubMed: 8301368]

Felder RB, Francis J, Zhang ZH, Wei SG, Weiss RM, Johnson AK. Heart failure and the brain: new perspectives. Am J Physiol Regul Integr Comp Physiol. 2003; 284:R259–276. [PubMed: 12529279]

Ferguson AV, Latchford KJ, Samson WK. The paraventricular nucleus of the hypothalamus - a potential target for integrative treatment of autonomic dysfunction. Expert Opin Ther Targets. 2008; 12:717–727. [PubMed: 18479218]

Fox EA, Powley TL. Longitudinal columnar organization within the dorsal motor nucleus represents separate branches of the abdominal vagus. Brain Res. 1985; 341:269–282. [PubMed: 4041795]

Gaykema RP, Chen CC, Goehler LE. Organization of immune-responsive medullary projections to the bed nucleus of the stria terminalis, central amygdala, and paraventricular nucleus of the hypothalamus: evidence for parallel viscerosensory pathways in the rat brain. Brain Res. 2007; 1130:130–145. [PubMed: 17169348]

Geerling JC, Engeland WC, Kawata M, Loewy AD. Aldosterone target neurons in the nucleus tractus solitarius drive sodium appetite. J Neurosci. 2006a; 26:411–417. [PubMed: 16407537]

Geerling JC, Kawata M, Loewy AD. Aldosterone-sensitive neurons in the rat central nervous system. J Comp Neurol. 2006b; 494:515–527. [PubMed: 16320254]

Geerling JC, Loewy AD. Aldosterone-sensitive neurons in the nucleus of the solitary tract: bidirectional connections with the central nucleus of the amygdala. J Comp Neurol. 2006a; 497:646–657. [PubMed: 16739197]

Geerling JC, Loewy AD. Aldosterone-sensitive neurons in the nucleus of the solitary: efferent projections. J Comp Neurol. 2006b; 498:223–250. [PubMed: 16933386]

Geerling JC, Loewy AD. Sodium depletion activates the aldosterone-sensitive neurons in the NTS independently of thirst. Am J Physiol Regul Integr Comp Physiol. 2007a; 292:R1338–1348. [PubMed: 17068161]

Geerling JC, Loewy AD. Sodium deprivation and salt intake activate separate neuronal subpopulations in the nucleus of the solitary tract and the parabrachial complex. J Comp Neurol. 2007b; 504:379–403. [PubMed: 17663450]

Geerling JC, Loewy AD. Central regulation of sodium appetite. Exp Physiol. 2008; 93:178–209.

Gerald C, Walker MW, Criscione L, Gustafson EL, Batzl-Hartmann C, Smith KE, Vaysse P, Durkin MM, Laz TM, Linemeyer DL, Schaffhauser AO, Whitebread S, Hofbauer KG, Taber RI, Branchek TA, Weinshank RL. A receptor subtype involved in neuropeptide-Y-induced food intake. Nature. 1996; 382:168–171. [PubMed: 8700207]

Gerfen CR, Sawchenko PE. A method for anterograde axonal tracing of chemically specified circuits in the central nervous system: combined Phaseolus vulgaris-leucoagglutinin (PHA-L) tract tracing and immunohistochemistry. Brain Res. 1985; 343:144–150. [PubMed: 3899276]

Goldman CK, Marino L, Leibowitz SF. Postsynaptic alpha 2-noradrenergic receptors mediate feeding induced by paraventricular nucleus injection of norepinephrine and clonidine. Eur J Pharmacol. 1985; 115:11–19. [PubMed: 2995083]

Gomez-Sanchez EP, Ganjam V, Chen YJ, Liu Y, Clark SA, Gomez-Sanchez CE. The 11beta hydroxysteroid dehydrogenase 2 exists as an inactive dimer. Steroids. 2001; 66:845–848. [PubMed: 11576624]

Goodchild AK, Moon EA. Maps of cardiovascular and respiratory regions of rat ventral medulla: Focus on the caudal medulla. J Chem Neuroanat. 2009

Gordon FJ, McCann LA. Pressor responses evoked by microinjections of L-glutamate into the caudal ventrolateral medulla of the rat. Brain Res. 1988; 457:251–258. [PubMed: 2905917]

Guyenet PG. The sympathetic control of blood pressure. Nat Rev Neurosci. 2006; 7:335–346. [PubMed: 16760914]

Guyenet PG. The 2008 Carl Ludwig Lecture: retrotrapezoid nucleus, CO2 homeostasis, and breathing automaticity. J Appl Physiol. 2008; 105:404–416. [PubMed: 18535135]

Haan EA, Jennings IG, Cuello AC, Nakata H, Fujisawa H, Chow CW, Kushinsky R, Brittingham J, Cotton RG. Identification of serotonergic neurons in human brain by a monoclonal antibody binding to all three aromatic amino acid hydroxylases. Brain Res. 1987; 426:19–27. [PubMed: 2891407]

Hara H, Hamill GS, Jacobowitz DM. Origin of cholinergic nerves to the rat major cerebral arteries: coexistence with vasoactive intestinal polypeptide. Brain Res Bull. 1985; 14:179–188. [PubMed: 3888351]

Hasue RH, Shammah-Lagnado SJ. Origin of the dopaminergic innervation of the central extended amygdala and accumbens shell: a combined retrograde tracing and immunohistochemical study in the rat. J Comp Neurol. 2002; 454:15–33. [PubMed: 12410615]

Hathout GM, Bhidayasiri R. Midbrain ataxia: an introduction to the mesencephalic locomotor region and the pedunculopontine nucleus. AJR Am J Roentgenol. 2005; 184:953–956. [PubMed: 15728623]

Hayakawa T, Zheng JQ, Yajima Y. Direct synaptic projections to esophageal motoneurons in the nucleus ambiguus from the nucleus of the solitary tract of the rat. J Comp Neurol. 1997; 381:18–30. [PubMed: 9087416]

Herbert H, Moga MM, Saper CB. Connections of the parabrachial nucleus with the nucleus of the solitary tract and the medullary reticular formation in the rat. J Comp Neurol. 1990; 293:540–580. [PubMed: 1691748]

Herman JP, Cullinan WE. Neurocircuitry of stress: central control of the hypothalamo-pituitary-adrenocortical axis. Trends Neurosci. 1997; 20:78–84. [PubMed: 9023876]

Hermanson O, Blomqvist A. Subnuclear localization of FOS-like immunoreactivity in the rat parabrachial nucleus after nociceptive stimulation. J Comp Neurol. 1996; 368:45–56. [PubMed: 8725293]

Hermes SM, Mitchell JL, Aicher SA. Most neurons in the nucleus tractus solitarii do not send collateral projections to multiple autonomic targets in the rat brain. Exp Neurol. 2006; 198:539–551. [PubMed: 16487517]

Higgins GA, Hoffman GE, Wray S, Schwaber JS. Distribution of neurotensin-immunoreactivity within baroreceptive portions of the nucleus of the tractus solitarius and the dorsal vagal nucleus of the rat. J Comp Neurol. 1984; 226:155–164. [PubMed: 6376547]

Hochstenbach SL, Ciriello J. Plasma hypernatremia induces c-fos activity in medullary catecholaminergic neurons. Brain Res. 1995; 674:46–54. [PubMed: 7773694]

Hopkins DA. Ultrastructure and synaptology of the nucleus ambiguus in the rat: the compact formation. J Comp Neurol. 1995; 360:705–725. [PubMed: 8801261]

Hopkins DA, Bieger D, deVente J, Steinbusch WM. Vagal efferent projections: viscerotopy, neurochemistry and effects of vagotomy. Prog Brain Res. 1996; 107:79–96. [PubMed: 8782514]

Horiuchi J, Dampney RA. Evidence for tonic disinhibition of RVLM sympathoexcitatory neurons from the caudal pressor area. Auton Neurosci. 2002; 99:102–110. [PubMed: 12241084]

Hosoya Y, Matsushita M. Identification and distribution of the spinal and hypophyseal projection neurons in the paraventricular nucleus of the rat. A light and electron microscopic study with the horseradish peroxidase method. Exp Brain Res. 1979; 35:315–331. [PubMed: 86456]

Hosoya Y, Matsushita M, Sugiura Y. A direct hypothalamic projection to the superior salivatory nucleus neurons in the rat. A study using anterograde autoradiographic and retrograde HRP methods. Brain Res. 1983; 266:329–333. [PubMed: 6191826]

Hosoya Y, Sugiura Y, Ito R, Kohno K. Descending projections from the hypothalamic paraventricular nucleus to the A5 area, including the superior salivatory nucleus, in the rat. Exp Brain Res. 1990; 82:513–518. [PubMed: 2292271]

Housley GD, Martin-Body RL, Dawson NJ, Sinclair JD. Brain stem projections of the glossopharyngeal nerve and its carotid sinus branch in the rat. Neuroscience. 1987; 22:237–250. [PubMed: 3627444]

Iigaya K, Kumagai H, Onimaru H, Kawai A, Oshima N, Onami T, Takimoto C, Kamayachi T, Hayashi K, Saruta T, Itoh H. Novel axonal projection from the caudal end of the ventrolateral medulla to the intermediolateral cell column. Am J Physiol Regul Integr Comp Physiol. 2007; 292:R927–936. [PubMed: 17082356]

Jansen AS, Loewy AD. Neurons lying in the white matter of the upper cervical spinal cord project to the intermediolateral cell column. Neuroscience. 1997; 77:889–898. [PubMed: 9070760]

Jennings IG, Russell RG, Armarego WL, Cotton RG. Functional analysis of the effect of monoclonal antibodies on monkey liver phenylalanine hydroxylase. Biochem J. 1986; 235:133–138. [PubMed: 2427069]

Kalra SP, Dube MG, Fournier A, Kalra PS. Structure-function analysis of stimulation of food intake by neuropeptide Y: effects of receptor agonists. Physiol Behav. 1991; 50:5–9. [PubMed: 1658831]

Kannan H, Hayashida Y, Yamashita H. Increase in sympathetic outflow by paraventricular nucleus stimulation in awake rats. Am J Physiol. 1989; 256:R1325–1330. [PubMed: 2567578]

Karimnamazi H, Travers SP, Travers JB. Oral and gastric input to the parabrachial nucleus of the rat. Brain Res. 2002; 957:193–206. [PubMed: 12445962]

Katafuchi T, Oomura Y, Kurosawa M. Effects of chemical stimulation of paraventricular nucleus on adrenal and renal nerve activity in rats. Neurosci Lett. 1988; 86:195–200. [PubMed: 2897095]

Kc P, Haxhiu MA, Tolentino-Silva FP, Wu M, Trouth CO, Mack SO. Paraventricular vasopressin-containing neurons project to brain stem and spinal cord respiratory-related sites. Respir Physiol Neurobiol. 2002; 133:75–88. [PubMed: 12385733]

Laughton WB, Powley TL. Localization of efferent function in the dorsal motor nucleus of the vagus. Am J Physiol. 1987; 252:R13–25. [PubMed: 3544872]

Leibowitz SF. Pattern of drinking and feeding produced by hypothalamic norepinephrine injection in the satiated rat. Physiol Behav. 1975; 14:731–742. [PubMed: 1187829]

Leibowitz SF. Paraventricular nucleus: a primary site mediating adrenergic stimulation of feeding and drinking. Pharmacol Biochem Behav. 1978; 8:163–175. [PubMed: 652826]

Leibowitz SF, Hammer NJ, Chang K. Hypothalamic paraventricular nucleus lesions produce overeating and obesity in the rat. Physiol Behav. 1981; 27:1031–1040. [PubMed: 7335803]

Leibowitz SF, Hammer NJ, Chang K. Feeding behavior induced by central norepinephrine injection is attenuated by discrete lesions in the hypothalamic paraventricular nucleus. Pharmacol Biochem Behav. 1983; 19:945–950. [PubMed: 6657727]

Leibowitz SF, Shor-Posner G, Brennan G, Alexander JT. Meal pattern analysis of macronutrient intake after PVN norepinephrine and peripheral clonidine administration. Obes Res. 1993; 1:29–39. [PubMed: 16353348]

Li HY, Ericsson A, Sawchenko PE. Distinct mechanisms underlie activation of hypothalamic neurosecretory neurons and their medullary catecholaminergic afferents in categorically different stress paradigms. Proc Natl Acad Sci U S A. 1996; 93:2359–2364. [PubMed: 8637878]

Li Q, Goodchild AK, Seyedabadi M, Pilowsky PM. Pre-protachykinin A mRNA is colocalized with tyrosine hydroxylase-immunoreactivity in bulbospinal neurons. Neuroscience. 2005; 136:205–216. [PubMed: 16198496]

Li YF, Patel KP. Paraventricular nucleus of the hypothalamus and elevated sympathetic activity in heart failure: the altered inhibitory mechanisms. Acta Physiol Scand. 2003; 177:17–26. [PubMed: 12492775]

Lima D, Albino-Teixeira A, Tavares I. The caudal medullary ventrolateral reticular formation in nociceptive-cardiovascular integration. An experimental study in the rat. Exp Physiol. 2002; 87:267–274. [PubMed: 11856973]

Lipski J, Kanjhan R, Kruszewska B, Smith M. Barosensitive neurons in the rostral ventrolateral medulla of the rat in vivo: morphological properties and relationship to C1 adrenergic neurons. Neuroscience. 1995; 69:601–618. [PubMed: 8552253]

Loeschcke HH. Central chemosensitivity and the reaction theory. J Physiol. 1982; 332:1–24. [PubMed: 6818338]

Loewy AD, McKellar S. Serotonergic projections from the ventral medulla to the intermediolateral cell column in the rat. Brain Res. 1981; 211:146–152. [PubMed: 6164449]

Lu J, Jhou TC, Saper CB. Identification of wake-active dopaminergic neurons in the ventral periaqueductal gray matter. J Neurosci. 2006a; 26:193–202. [PubMed: 16399687]

Lu J, Sherman D, Devor M, Saper CB. A putative flip-flop switch for control of REM sleep. Nature. 2006b; 441:589–594. [PubMed: 16688184]

Luiten PG, ter Horst GJ, Karst H, Steffens AB. The course of paraventricular hypothalamic efferents to autonomic structures in medulla and spinal cord. Brain Res. 1985; 329:374–378. [PubMed: 3978460]

Mack SO, Kc P, Wu M, Coleman BR, Tolentino-Silva FP, Haxhiu MA. Paraventricular oxytocin neurons are involved in neural modulation of breathing. J Appl Physiol. 2002; 92:826–834. [PubMed: 11796698]

Mack SO, Wu M, Kc P, Haxhiu MA. Stimulation of the hypothalamic paraventricular nucleus modulates cardiorespiratory responses via oxytocinergic innervation of neurons in pre-Botzinger complex. J Appl Physiol. 2007; 102:189–199. [PubMed: 16857863]

Martin DS, Segura T, Haywood JR. Cardiovascular responses to bicuculline in the paraventricular nucleus of the rat. Hypertension. 1991; 18:48–55. [PubMed: 1860711]

Mayne RG, Armstrong WE, Crowley WR, Bealer SL. Cytoarchitectonic analysis of Fos-immunoreactivity in brainstem neurones following visceral stimuli in conscious rats. J Neuroendocrinol. 1998; 10:839–847. [PubMed: 9831260]

McAllen RM, Spyer KM. The location of cardiac vagal preganglionic motoneurones in the medulla of the cat. J Physiol. 1976; 258:187–204. [PubMed: 940054]

McAllen RM, Spyer KM. Two types of vagal preganglionic motoneurones projecting to the heart and lungs. J Physiol. 1978; 282:353–364. [PubMed: 722537]

McCabe JT, DeBellis M, Leibowitz SF. Clonidine-induced feeding: analysis of central sites of action and fiber projections mediating this response. Brain Res. 1984; 309:85–104. [PubMed: 6488015]

McCulloch PF, Panneton WM. Fos immunohistochemical determination of brainstem neuronal activation in the muskrat after nasal stimulation. Neuroscience. 1997; 78:913–925. [PubMed: 9153669]

Millhorn DE, Hokfelt T, Seroogy K, Oertel W, Verhofstad AA, Wu JY. Immunohistochemical evidence for colocalization of gamma-aminobutyric acid and serotonin in neurons of the ventral medulla oblongata projecting to the spinal cord. Brain Res. 1987; 410:179–185. [PubMed: 3555707]

Moga MM, Herbert H, Hurley KM, Yasui Y, Gray TS, Saper CB. Organization of cortical, basal forebrain, and hypothalamic afferents to the parabrachial nucleus in the rat. J Comp Neurol. 1990; 295:624–661. [PubMed: 1694187]

Moore SD, Guyenet PG. An electrophysiological study of the forebrain projection of nucleus commissuralis: preliminary identification of presumed A2 catecholaminergic neurons. Brain Res. 1983; 263:211–222. [PubMed: 6301647]

Morrison SF, Cao WH. Different adrenal sympathetic preganglionic neurons regulate epinephrine and norepinephrine secretion. Am J Physiol Regul Integr Comp Physiol. 2000; 279:R1763–1775. [PubMed: 11049860]

Mulkey DK, Stornetta RL, Weston MC, Simmons JR, Parker A, Bayliss DA, Guyenet PG. Respiratory control by ventral surface chemoreceptor neurons in rats. Nat Neurosci. 2004; 7:1360–1369. [PubMed: 15558061]

Nakai M, Tamaki K, Ogata J, Matsui Y, Maeda M. Parasympathetic cerebrovasodilator center of the facial nerve. Circ Res. 1993; 72:470–475. [PubMed: 8093431]

Nakamura K, Morrison SF. A thermosensory pathway that controls body temperature. Nat Neurosci. 2008; 11:62–71. [PubMed: 18084288]

Naray-Fejes-Toth A, Fejes-Toth G. Subcellular localization of the type 2 11beta-hydroxysteroid dehydrogenase. A green fluorescent protein study. J Biol Chem. 1996; 271:15436–15442. [PubMed: 8663122]

Naray-Fejes-Toth A, Fejes-Toth G. Extranuclear localization of endogenous 11beta-hydroxysteroid dehydrogenase-2 in aldosterone target cells. Endocrinology. 1998; 139:2955–2959. [PubMed: 9607806]

Natarajan M, Morrison SF. Sympathoexcitatory CVLM neurons mediate responses to caudal pressor area stimulation. Am J Physiol Regul Integr Comp Physiol. 2000; 279:R364–374. [PubMed: 10938222]

Nattie EE, Li A. Substance P-saporin lesion of neurons with NK1 receptors in one chemoreceptor site in rats decreases ventilation and chemosensitivity. J Physiol. 2002; 544:603–616. [PubMed: 12381830]

Norgren R, Smith GP. Central distribution of subdiaphragmatic vagal branches in the rat. J Comp Neurol. 1988; 273:207–223. [PubMed: 3417902]

Odermatt A, Arnold P, Stauffer A, Frey BM, Frey FJ. The N-terminal anchor sequences of 11beta-hydroxysteroid dehydrogenases determine their orientation in the endoplasmic reticulum membrane. J Biol Chem. 1999; 274:28762–28770. [PubMed: 10497248]

Ohiwa N, Saito T, Chang H, Omori T, Fujikawa T, Asada T, Soya H. Activation of A1 and A2 noradrenergic neurons in response to running in the rat. Neurosci Lett. 2006; 395:46–50. [PubMed: 16293368]

Okada Y, Chen Z, Kuwana S. Cytoarchitecture of central chemoreceptors in the mammalian ventral medulla. Respir Physiol. 2001; 129:13–23. [PubMed: 11738643]

Okamura T, Ayajiki K, Fujioka H, Shinozaki K, Toda N. Neurogenic cerebral vasodilation mediated by nitric oxide. Jpn J Pharmacol. 2002; 88:32–38. [PubMed: 11855675]

Onaka T, Luckman SM, Antonijevic I, Palmer JR, Leng G. Involvement of the noradrenergic afferents from the nucleus tractus solitarii to the supraoptic nucleus in oxytocin release after peripheral cholecystokinin octapeptide in the rat. Neuroscience. 1995; 66:403–412. [PubMed: 7477881]

Pan B, Castro-Lopes JM, Coimbra A. Central afferent pathways conveying nociceptive input to the hypothalamic paraventricular nucleus as revealed by a combination of retrograde labeling and c-fos activation. J Comp Neurol. 1999; 413:129–145. [PubMed: 10464375]

Panneton WM, McCulloch PF, Sun W. Trigemino-autonomic connections in the muskrat: the neural substrate for the diving response. Brain Res. 2000; 874:48–65. [PubMed: 10936223]

Paterson DS, Thompson EG, Kinney HC. Serotonergic and glutamatergic neurons at the ventral medullary surface of the human infant: Observations relevant to central chemosensitivity in early human life. Auton Neurosci. 2006; 124:112–124. [PubMed: 16458076]

Paxinos, G.; Watson, C. The Rat Brain in Stereotaxic Coordinates. Elsevier; Burlington, MA: 1998.

Petrovich GD, Swanson LW. Projections from the lateral part of the central amygdalar nucleus to the postulated fear conditioning circuit. Brain Res. 1997; 763:247–254. [PubMed: 9296566]

Pilowsky P, Llewellyn-Smith IJ, Arnolda L, Lipski J, Minson J, Chalmers J. Are the ventrally projecting dendrites of respiratory neurons a neuroanatomical basis for the chemosensitivity of the ventral medulla oblongata? Sleep. 1993; 16:S53–55. [PubMed: 8178025]

Pilowsky PM, Jiang C, Lipski J. An intracellular study of respiratory neurons in the rostral ventrolateral medulla of the rat and their relationship to catecholamine-containing neurons. J Comp Neurol. 1990; 301:604–617. [PubMed: 1980279]

Possas OS, Campos RR Jr. Cravo SL, Lopes OU, Guertzenstein PG. A fall in arterial blood pressure produced by inhibition of the caudalmost ventrolateral medulla: the caudal pressor area. J Auton Nerv Syst. 1994; 49:235–245. [PubMed: 7806775]

Powley, TL.; Berthoud, H-R.; Fox, EA.; Laughton, WB. The dorsal vagal complex forms a sensory-motor lattice: the circuitry of gastrointestinal reflexes. In: Ritter, S.; Ritter, R.; Barnes, C.,

editors. Neuroanatomy and Physiology of Abdominal Vagal Afferents. CRC Press; Boca Raton, FL: 1992. p. 57-79.

Pyner S, Coote JH. Identification of an efferent projection from the paraventricular nucleus of the hypothalamus terminating close to spinally projecting rostral ventrolateral medullary neurons. Neuroscience. 1999; 88:949–957. [PubMed: 10363830]

Pyner S, Coote JH. Identification of branching paraventricular neurons of the hypothalamus that project to the rostroventrolateral medulla and spinal cord. Neuroscience. 2000; 100:549–556. [PubMed: 11098118]

Reyes BA, Valentino RJ, Xu G, Van Bockstaele EJ. Hypothalamic projections to locus coeruleus neurons in rat brain. Eur J Neurosci. 2005; 22:93–106. [PubMed: 16029199]

Richard S, Engblom D, Paues J, Mackerlova L, Blomqvist A. Activation of the parabrachio-amygdaloid pathway by immune challenge or spinal nociceptive input: a quantitative study in the rat using Fos immunohistochemistry and retrograde tract tracing. J Comp Neurol. 2005; 481:210–219. [PubMed: 15562506]

Rinaman L, Card JP, Schwaber JS, Miselis RR. Ultrastructural demonstration of a gastric monosynaptic vagal circuit in the nucleus of the solitary tract in rat. J Neurosci. 1989; 9:1985–1996. [PubMed: 2723763]

Ritter RC, Epstein AN. Control of meal size by central noradrenergic action. Proc Natl Acad Sci U S A. 1975; 72:3740–3743. [PubMed: 1059162]

Ritter S, Bugarith K, Dinh TT. Immunotoxic destruction of distinct catecholamine subgroups produces selective impairment of glucoregulatory responses and neuronal activation. J Comp Neurol. 2001; 432:197–216. [PubMed: 11241386]

Ritter S, Llewellyn-Smith I, Dinh TT. Subgroups of hindbrain catecholamine neurons are selectively activated by 2-deoxy-D-glucose induced metabolic challenge. Brain Res. 1998; 805:41–54. [PubMed: 9733914]

Ritter S, Watts AG, Dinh TT, Sanchez-Watts G, Pedrow C. Immunotoxin lesion of hypothalamically projecting norepinephrine and epinephrine neurons differentially affects circadian and stressor-stimulated corticosterone secretion. Endocrinology. 2003; 144:1357–1367. [PubMed: 12639919]

Roder S, Ciriello J. Innervation of the amygdaloid complex by catecholaminergic cell groups of the ventrolateral medulla. J Comp Neurol. 1993; 332:105–122. [PubMed: 7685779]

Rogers RC, Hermann GE. Gastric-vagal solitary neurons excited by paraventricular nucleus microstimulation. J Auton Nerv Syst. 1985; 14:351–362. [PubMed: 4086724]

Roland BL, Krozowski ZS, Funder JW. Glucocorticoid receptor, mineralocorticoid receptors, 11 beta-hydroxysteroid dehydrogenase-1 and -2 expression in rat brain and kidney: in situ studies. Mol Cell Endocrinol. 1995a; 111:R1–7. [PubMed: 7649347]

Roland BL, Li KX, Funder JW. Hybridization histochemical localization of 11 beta-hydroxysteroid dehydrogenase type 2 in rat brain. Endocrinology. 1995b; 136:4697–4700. [PubMed: 7664691]

Roland BL, Sawchenko PE. Local origins of some GABAergic projections to the paraventricular and supraoptic nuclei of the hypothalamus in the rat. J Comp Neurol. 1993; 332:123–143. [PubMed: 7685780]

Rosin DL, Chang DA, Guyenet PG. Afferent and efferent connections of the rat retrotrapezoid nucleus. J Comp Neurol. 2006; 499:64–89. [PubMed: 16958085]

Ross CA, Ruggiero DA, Park DH, Joh TH, Sved AF, Fernandez-Pardal J, Saavedra JM, Reis DJ. Tonic vasomotor control by the rostral ventrolateral medulla: effect of electrical or chemical stimulation of the area containing C1 adrenaline neurons on arterial pressure, heart rate, and plasma catecholamines and vasopressin. J Neurosci. 1984; 4:474–494. [PubMed: 6699683]

Saper CB, Loewy AD, Swanson LW, Cowan WM. Direct hypothalamo-autonomic connections. Brain Res. 1976; 117:305–312. [PubMed: 62600]

Sartor DM, Verberne AJ. Cholecystokinin selectively affects presympathetic vasomotor neurons and sympathetic vasomotor outflow. Am J Physiol Regul Integr Comp Physiol. 2002; 282:R1174–1184. [PubMed: 11893623]

Sato M, Severinghaus JW, Basbaum AI. Medullary CO2 chemoreceptor neuron identification by c-fos immunocytochemistry. J Appl Physiol. 1992; 73:96–100. [PubMed: 1506406]

Sawchenko PE, Brown ER, Chan RK, Ericsson A, Li HY, Roland BL, Kovacs KJ. The paraventricular nucleus of the hypothalamus and the functional neuroanatomy of visceromotor responses to stress. Prog Brain Res. 1996; 107:201–222. [PubMed: 8782521]

Sawchenko PE, Gold RM, Leibowitz SF. Evidence for vagal involvement in the eating elicited by adrenergic stimulation of the paraventricular nucleus. Brain Res. 1981; 225:249–269. [PubMed: 7030452]

Sawchenko PE, Swanson LW. Immunohistochemical identification of neurons in the paraventricular nucleus of the hypothalamus that project to the medulla or to the spinal cord in the rat. J Comp Neurol. 1982a; 205:260–272. [PubMed: 6122696]

Sawchenko PE, Swanson LW. The organization of noradrenergic pathways from the brainstem to the paraventricular and supraoptic nuclei in the rat. Brain Res. 1982b; 257:275–325. [PubMed: 6756545]

Sawchenko PE, Swanson LW, Grzanna R, Howe PR, Bloom SR, Polak JM. Colocalization of neuropeptide Y immunoreactivity in brainstem catecholaminergic neurons that project to the paraventricular nucleus of the hypothalamus. J Comp Neurol. 1985; 241:138–153. [PubMed: 3840810]

Saxon DW, Hopkins DA. Ultrastructure and synaptology of the paratrigeminal nucleus in the rat: primary pharyngeal and laryngeal afferent projections. Synapse. 2006; 59:220–234. [PubMed: 16385507]

Seyedabadi M, Li Q, Padley JR, Pilowsky PM, Goodchild AK. A novel pressor area at the medullo-cervical junction that is not dependent on the RVLM: efferent pathways and chemical mediators. J Neurosci. 2006; 26:5420–5427. [PubMed: 16707794]

Shafton AD, Ryan A, Badoer E. Neurons in the hypothalamic paraventricular nucleus send collaterals to the spinal cord and to the rostral ventrolateral medulla in the rat. Brain Res. 1998; 801:239–243. [PubMed: 9729407]

Shapiro RE, Miselis RR. The central organization of the vagus nerve innervating the stomach of the rat. J Comp Neurol. 1985; 238:473–488. [PubMed: 3840183]

Shin JW, Geerling JC, Loewy AD. Inputs to the ventrolateral bed nucleus of the stria terminalis. J Comp Neurol. 2008; 511:628–657. [PubMed: 18853414]

Shor-Posner G, Azar AP, Volpe M, Grinker JA, Leibowitz SF. Clonidine hyperphagia: neuroanatomic substrates and specific function. Pharmacol Biochem Behav. 1988; 30:925–932. [PubMed: 3147461]

Sita LV, Elias CF, Bittencourt JC. Connectivity pattern suggests that incerto-hypothalamic area belongs to the medial hypothalamic system. Neuroscience. 2007; 148:949–969. [PubMed: 17707116]

Smith DW, Buller KM, Day TA. Role of ventrolateral medulla catecholamine cells in hypothalamic neuroendocrine cell responses to systemic hypoxia. J Neurosci. 1995; 15:7979–7988. [PubMed: 8613735]

South EH, Ritter RC. Overconsumption of preferred foods following capsaicin pretreatment of the area postrema and adjacent nucleus of the solitary tract. Brain Res. 1983; 288:243–251. [PubMed: 6661619]

Spencer SE, Sawyer WB, Wada H, Platt KB, Loewy AD. CNS projections to the pterygopalatine parasympathetic preganglionic neurons in the rat: a retrograde transneuronal viral cell body labeling study. Brain Res. 1990; 534:149–169. [PubMed: 1705849]

Stanley BG, Leibowitz SF. Neuropeptide Y injected in the paraventricular hypothalamus: a powerful stimulant of feeding behavior. Proc Natl Acad Sci U S A. 1985; 82:3940–3943. [PubMed: 3858854]

Steininger TL, Rye DB, Wainer BH. Afferent projections to the cholinergic pedunculopontine tegmental nucleus and adjacent midbrain extrapyramidal area in the albino rat. I. Retrograde tracing studies. J Comp Neurol. 1992; 321:515–543. [PubMed: 1380518]

Stocker SD, Cunningham JT, Toney GM. Water deprivation increases Fos immunoreactivity in PVN autonomic neurons with projections to the spinal cord and rostral ventrolateral medulla. Am J Physiol Regul Integr Comp Physiol. 2004; 287:R1172–1183. [PubMed: 15271657]

Stocker SD, Simmons JR, Stornetta RL, Toney GM, Guyenet PG. Water deprivation activates a glutamatergic projection from the hypothalamic paraventricular nucleus to the rostral ventrolateral medulla. J Comp Neurol. 2006; 494:673–685. [PubMed: 16374796]

Stornetta RL, Guyenet PG. Distribution of glutamic acid decarboxylase mRNA-containing neurons in rat medulla projecting to thoracic spinal cord in relation to monoaminergic brainstem neurons. J Comp Neurol. 1999; 407:367–380. [PubMed: 10320217]

Stornetta RL, Moreira TS, Takakura AC, Kang BJ, Chang DA, West GH, Brunet JF, Mulkey DK, Bayliss DA, Guyenet PG. Expression of Phox2b by brainstem neurons involved in chemosensory integration in the adult rat. J Neurosci. 2006; 26:10305–10314. [PubMed: 17021186]

Stuesse SL, Fish SE. Projections to the cardioinhibitory region of the nucleus ambiguus of rat. J Comp Neurol. 1984; 229:271–278. [PubMed: 6501603]

Subramanian HH, Balnave RJ, Holstege G. The midbrain periaqueductal gray control of respiration. J Neurosci. 2008; 28:12274–12283. [PubMed: 19020021]

Sugitani A, Yoshida J, Nyhus LM, Donahue PE. Viscerotopic representation of preganglionic efferent vagus nerve in the brainstem of the rat: a Fluoro-Gold study. J Auton Nerv Syst. 1991; 34:211–219. [PubMed: 1717538]

Sun QJ, Pilowsky P, Minson J, Arnolda L, Chalmers J, Llewellyn-Smith IJ. Close appositions between tyrosine hydroxylase immunoreactive boutons and respiratory neurons in the rat ventrolateral medulla. J Comp Neurol. 1994; 340:1–10. [PubMed: 7909820]

Sun W, Panneton WM. The caudal pressor area of the rat: its precise location and projections to the ventrolateral medulla. Am J Physiol Regul Integr Comp Physiol. 2002; 283:R768–778. [PubMed: 12185012]

Sun W, Panneton WM. Defining projections from the caudal pressor area of the caudal ventrolateral medulla. J Comp Neurol. 2005; 482:273–293. [PubMed: 15690490]

Swanson LW. Immunohistochemical evidence for a neurophysin-containing autonomic pathway arising in the paraventricular nucleus of the hypothalamus. Brain Res. 1977; 128:346–353. [PubMed: 301423]

Swanson, LW. Brain maps: structure of the rat brain. Elsevier; Amsterdam: 1998.

Swanson LW, Kuypers HG. The paraventricular nucleus of the hypothalamus: cytoarchitectonic subdivisions and organization of projections to the pituitary, dorsal vagal complex, and spinal cord as demonstrated by retrograde fluorescence double-labeling methods. J Comp Neurol. 1980; 194:555–570. [PubMed: 7451682]

Swanson LW, Sawchenko PE, Wiegand SJ, Price JL. Separate neurons in the paraventricular nucleus project to the median eminence and to the medulla or spinal cord. Brain Res. 1980; 198:190–195. [PubMed: 7407584]

Takakura AC, Moreira TS, Stornetta RL, West GH, Gwilt JM, Guyenet PG. Selective lesion of retrotrapezoid Phox2b-expressing neurons raises the apnoeic threshold in rats. J Physiol. 2008; 586:2975–2991. [PubMed: 18440993]

Talman WT, Corr J, Nitschke Dragon D, Wang D. Parasympathetic stimulation elicits cerebral vasodilatation in rat. Auton Neurosci. 2007; 133:153–157. [PubMed: 17275420]

Terenzi MG, Ingram CD. A combined immunocytochemical and retrograde tracing study of noradrenergic connections between the caudal medulla and bed nuclei of the stria terminalis. Brain Res. 1995; 672:289–297. [PubMed: 7749750]

Thompson RH, Swanson LW. Structural characterization of a hypothalamic visceromotor pattern generator network. Brain Res Brain Res Rev. 2003; 41:153–202. [PubMed: 12663080]

Toth ZE, Gallatz K, Fodor M, Palkovits M. Decussations of the descending paraventricular pathways to the brainstem and spinal cord autonomic centers. J Comp Neurol. 1999; 414:255–266. [PubMed: 10516595]

Van Bockstaele EJ, Chan J, Pickel VM. Input from central nucleus of the amygdala efferents to pericoerulear dendrites, some of which contain tyrosine hydroxylase immunoreactivity. J Neurosci Res. 1996; 45:289–302. [PubMed: 8841990]

Van Bockstaele EJ, Peoples J, Telegan P. Efferent projections of the nucleus of the solitary tract to peri-locus coeruleus dendrites in rat brain: evidence for a monosynaptic pathway. J Comp Neurol. 1999; 412:410–428. [PubMed: 10441230]

Van Bockstaele EJ, Pieribone VA, Aston-Jones G. Diverse afferents converge on the nucleus paragigantocellularis in the rat ventrolateral medulla: retrograde and anterograde tracing studies. J Comp Neurol. 1989; 290:561–584. [PubMed: 2482306]

Verbalis JG, McCann MJ, McHale CM, Stricker EM. Oxytocin secretion in response to cholecystokinin and food: differentiation of nausea from satiety. Science. 1986; 232:1417–1419. [PubMed: 3715453]

Waldbaum S, Hadziefendic S, Erokwu B, Zaidi SI, Haxhiu MA. CNS innervation of posterior cricoarytenoid muscles: a transneuronal labeling study. Respir Physiol. 2001; 126:113–125. [PubMed: 11348639]

Weese-Mayer DE, Berry-Kravis EM, Marazita ML. In pursuit (and discovery) of a genetic basis for congenital central hypoventilation syndrome. Respir Physiol Neurobiol. 2005; 149:73–82. [PubMed: 16054879]

Weston MC, Stornetta RL, Guyenet PG. Glutamatergic neuronal projections from the marginal layer of the rostral ventral medulla to the respiratory centers in rats. J Comp Neurol. 2004; 473:73–85. [PubMed: 15067719]

Woulfe JM, Flumerfelt BA, Hrycyshyn AW. Efferent connections of the A1 noradrenergic cell group: a DBH immunohistochemical and PHA-L anterograde tracing study. Exp Neurol. 1990; 109:308–322. [PubMed: 1976532]

Yamamoto T, Sawa K. c-Fos-like immunoreactivity in the brainstem following gastric loads of various chemical solutions in rats. Brain Res. 2000; 866:135–143. [PubMed: 10825489]

Yamashita H, Kannan H, Ueta Y. Involvement of caudal ventrolateral medulla neurons in mediating visceroreceptive information to the hypothalamic paraventricular nucleus. Prog Brain Res. 1989; 81:293–302. [PubMed: 2616788]

Yang Z, Coote JH. Influence of the hypothalamic paraventricular nucleus on cardiovascular neurones in the rostral ventrolateral medulla of the rat. J Physiol. 1998; 513(Pt 2):521–530. [PubMed: 9807000]

Zafra MA, Molina F, Puerto A. The neural/cephalic phase reflexes in the physiology of nutrition. Neurosci Biobehav Rev. 2006; 30:1032–1044. [PubMed: 16678262]

Zhang X, Fogel R, Renehan WE. Stimulation of the paraventricular nucleus modulates the activity of gut-sensitive neurons in the vagal complex. Am J Physiol. 1999; 277:G79–90. [PubMed: 10409154]

Zheng JQ, Seki M, Hayakawa T, Ito H, Zyo K. Descending projections from the paraventricular hypothalamic nucleus to the spinal cord: anterograde tracing study in the rat. Okajimas Folia Anat Jpn. 1995; 72:119–135. [PubMed: 8559555]

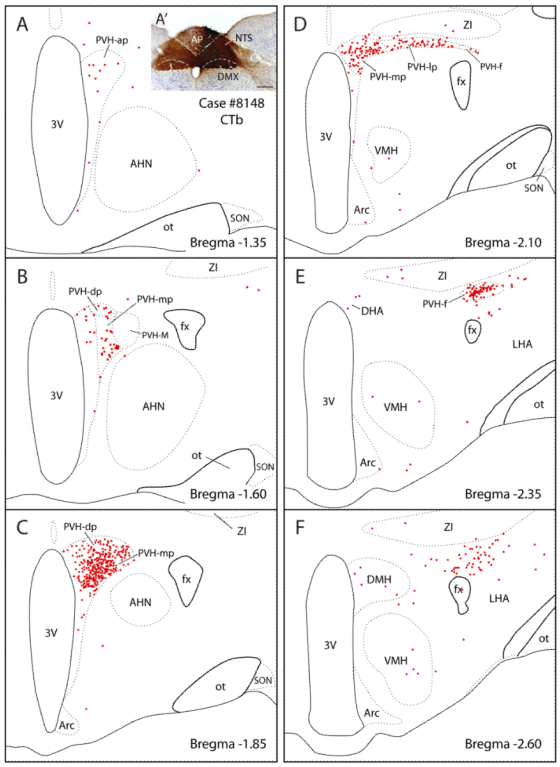


**Figure 1 A-F.**

Distribution of PVH neurons that project to the NTS as determined by retrograde neuronal labeling. CTb was injected in the medial NTS (insert panel **A′**), with some spread into the dorsal vagal nucleus (DMX) and area postrema (AP). This pattern of retrograde labeling is relevant to the present study because, among all target sites in the brainstem, this region of the NTS receives the most extensive input from the PVH. Most of the neurons that project to the NTS (red dots) are concentrated in a ventral region of the medial parvicellular PVH (PVH-mp, panel **C**), but other regions including the dorsal, lateral, and perifornical parvicellular subdivisions (PVH-dp, PVH-lp, and PVH-f, respectively) contribute to this projection. These projection neurons are not restricted to any one of PVH subdivision, but originate from all of regions, including the dorsal parvicellular subnucleus, which supplies the highest number of PVH neurons that project to the spinal cord (Hosoya and Matsushita, 1979). Weaker projections from contralateral PVH subnuclei were found as well. Very few CTb-labeled cells were located in surrounding regions of the diencephalon, other than a group of neurons lying dorsal to the fornix in the LHA (panel **F**), which is anatomically continuous with and morphologically similar to those in the PVH. Case #8148 was used in a previous publication (Geerling and Loewy, 2006a). Inset scale bar is 500 μm.

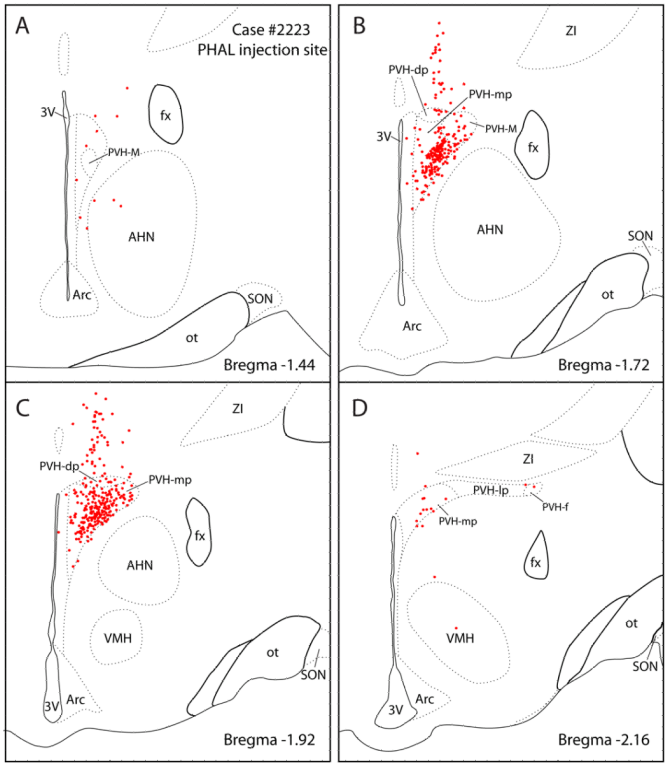


**Figure 2.**

PHAL injection site from case #2223 used to study the PVH projections to the brainstem. The axonal labeling in brainstem sections from this case is illustrated in Figure 4. Most labeled neurons (red dots) were concentrated in the medial parvicellular PVH subdivision (PVH-mp) and to lesser degree in the dorsal parvicellular subnuclei (PVH-dp). A few labeled cells were found in the lateral and forniceal parvicellular PVH subnuclei (PVH-lp and PVH-f). A scattering of labeled cells was also distributed dorsally along the pipette tract.

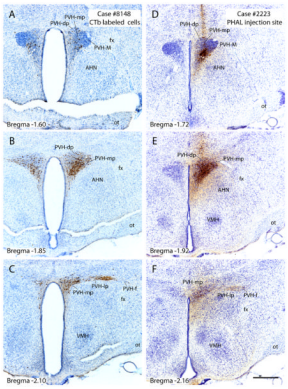


**Figure 3.**

Photoimages comparing the retrograde cell body labeling in the PVH following a CTb injection in the NTS (case# 8148; **A-C**) with a PHAL injection site localized in the medial parvicellular PVH region (case #2223; **D-F**). Drawings from these two cases are presented in Figures 1 & 2. Scale bar = 500 μm.

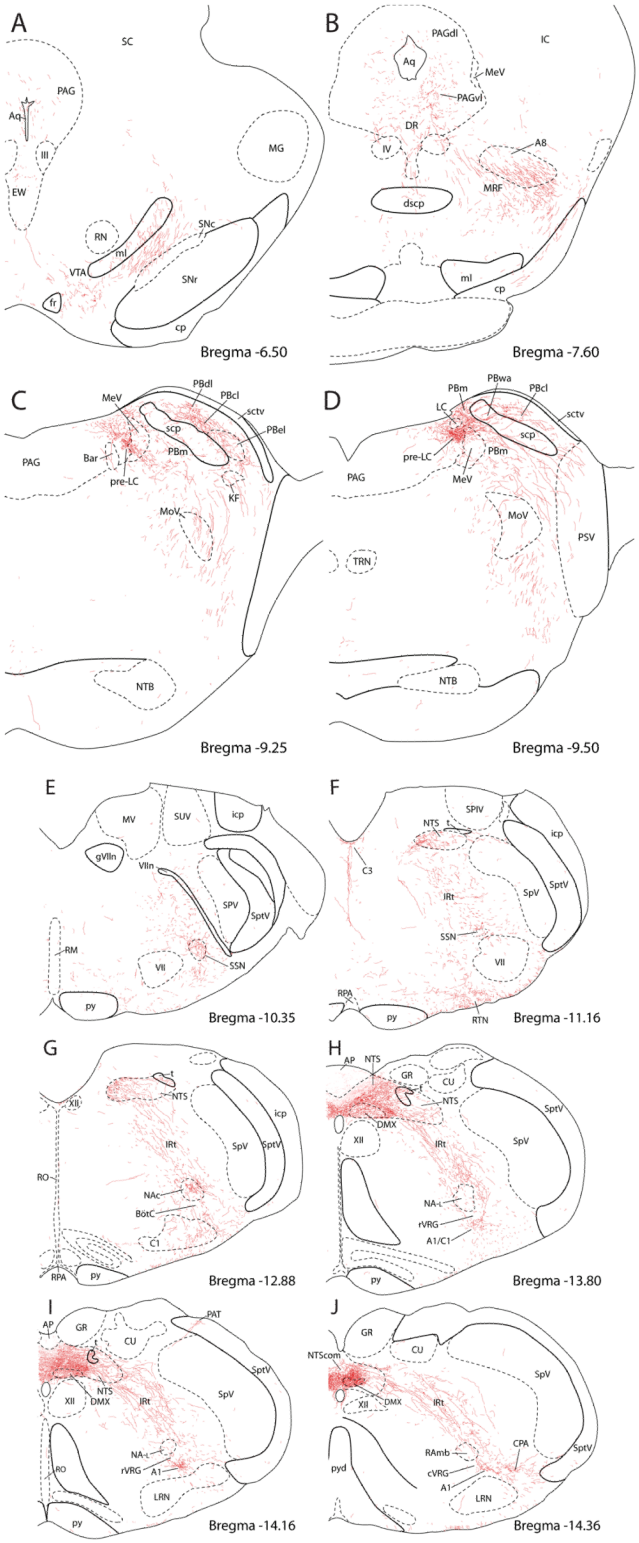


**Figure 4.**

PVH projections to the brainstem illustrated in a series of line drawings from the midbrain (**A and B**), pontine level (**C and D**), and medulla (**E-J**). See Figures 2 & 3 for injection site (case #2223).

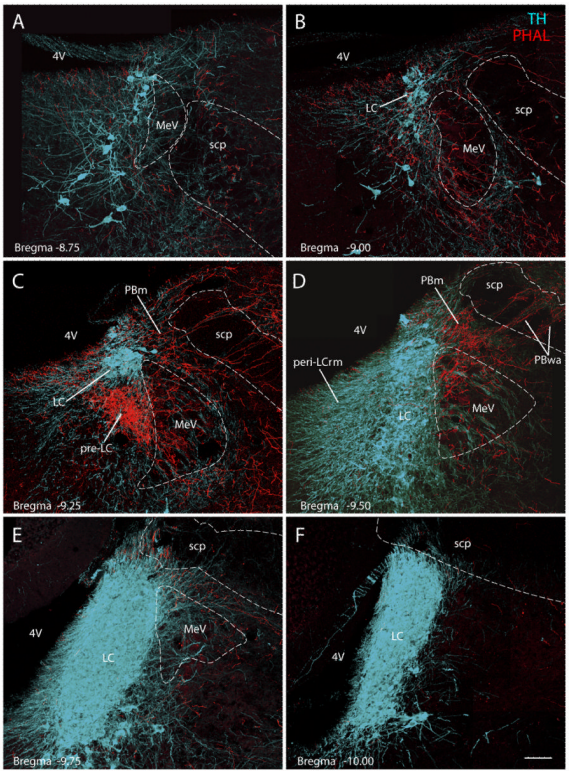


**Figure 5.**

Transverse images from the dorsolateral pons show PVH axons (red, PHAL) in the pre-locus coeruleus (pre-LC). These confocal montages were spaced 200μm apart and arranged from rostral (**A**) to caudal (**F**). Case #2223; see Figures 2 & 3 for injection site. The nuclear core of the LC (TH-immunoreactive neurons, ice-blue) contained minimal axonal labeling. Some varicose axons coursed through its perinuclear dendritic field (peri-LCrm) and the medial edge of the LC. Relative to the pre-LC and PBm, these perinuclear TH-labeled dendrites were not densely targeted, but when examined in individual confocal planes (not shown) some did appear to receive close contacts with PHAL-labeled boutons, consistent with prior electron microscopic observations (Reyes et al., 2005). Scale bar = 100 μm.

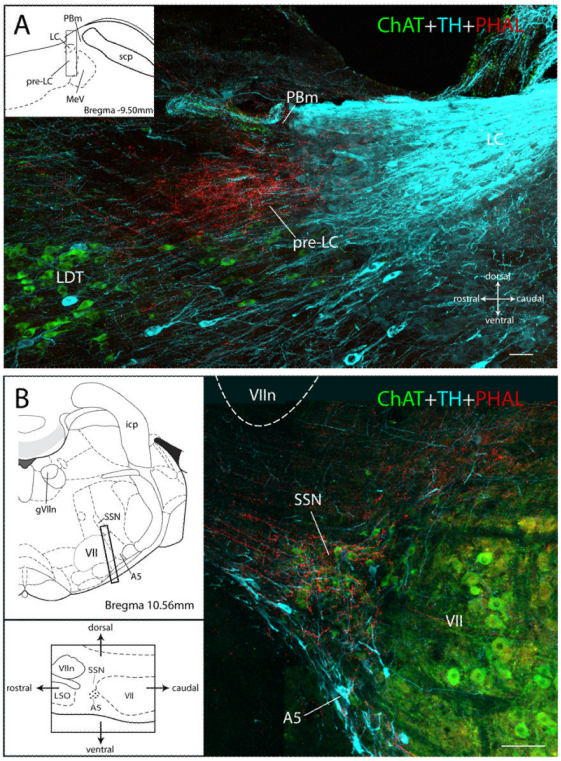


**Figure 6.**

(**A**) The PVH projects densely to the pre-locus coeruleus nucleus (pre-LC) (red, PHAL-immunoreactive axons), and not to the LC proper (ice-blue, TH-immunoreactive neurons) except for an occasional fiber as shown in this sagittal section. The region targeted by the PVH is also separate from the cholinergic neurons of the LDT (green) (Case #2697). Insert drawing showing the position and plane of this sagittal section. Scale bar = 100 μm.

(**B**) The PVH projection to the superior salivary nucleus (SSN) is shown in the sagittal plane (Case #2511; see Fig. 7 for injection site). The SSN contains a cluster of small, cholinergic parasympathetic preganglionic neurons (green, ChAT), centered just rostral and dorsolateral to the large motor neurons of the facial nucleus (VII, green labeled ChAT neurons) and bordered ventrally by A5 noradrenergic neurons (ice-blue, TH) running above the lateral superior olive. A few PVH axons were seen in the A5 noradrenergic cell group and an occasional fiber produced a small number of varicosities that contacted their TH-ir dendrites (not shown). Insert line drawing was adapted from Paxinos and Watson (1998) with modifications. Scale bar = 100 μm.

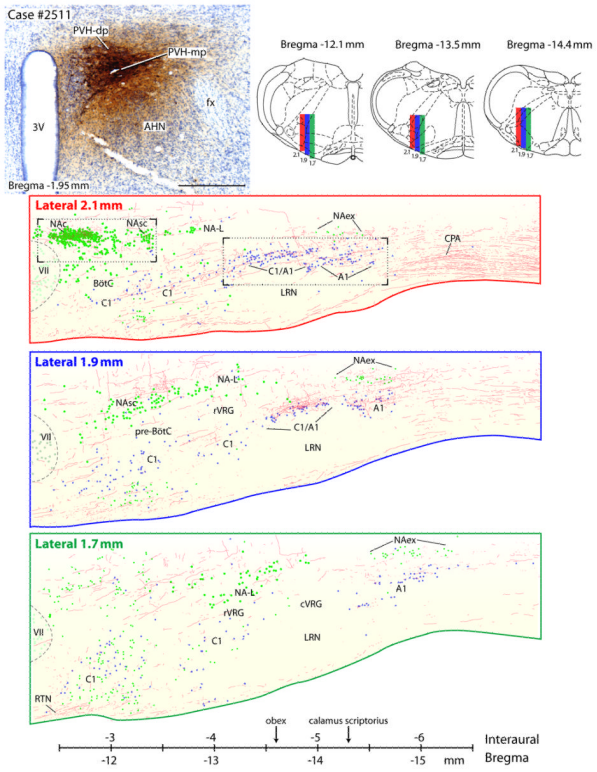


**Figure 7.**

The PVH projects to various neuronal cell groups of the ventrolateral medulla; these are presented as a series of three consecutive sections in the sagittal plane. Upper left panel shows the injection from case #2511. Upper right panel shows three transverse brainstem sections showing the plane of section where the sagittal slices were taken (Paxinos, 1998). Lower part of figure shows the PVH axonal labeling in reference to three defined cell groups: A1 and C1 catecholamine cell groups, nucleus ambiguus complex, and the respiratory nuclei (BötC = Bötzinger complex; cVRG = caudal ventral respiratory group; pre-BötC = pre-Bötzinger complex; rVRG = rostral ventral respiratory group - see reviews by (Alheid and McCrimmon, 2008; Goodchild and Moon, 2009). These drawings include all the PHAL-labeled axons and TH- or ChAT-labeled cells found in each of these 200 μm thick sagittal sections, which were complied from contiguous confocal images that were merged into a montage spanning the entire ventrolateral medulla. For anatomical reference, the large and distinct cholinergic motor neurons in the facial motor nucleus are represented by faint green dots. Motor neurons in the NAc, NAsc, and NA-L are shown as medium-sized green dots, and both the small parasympathetic motor neurons in the NAex and a poorly-characterized population of small cholinergic neurons within the rostral C1 region are represented by small green dots (green = ChAT-ir). Small blue dots represent catecholamine neurons in the C1 and A1 groups (TH-ir). Photoimages from the two areas outlined in the sagittal section from the Lateral 2.2 mm slice are presented in Figures 8 A & B. The scale bar was adapted from Paxinos and Watson (1998), using the caudal end of the facial nucleus as shown in the lateral 2.1 mm drawing as equal to -2.5 mm interaural level. The obex was located at the −4.6 mm interaural level and calamus scriptorius was at -5.3 mm interaural level.

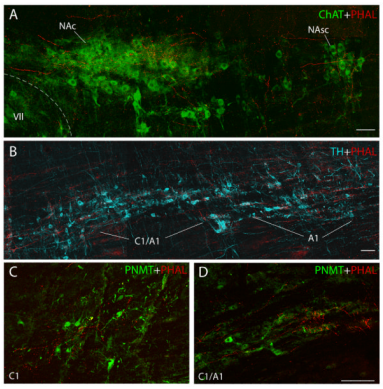


**Figure 8.**

**A.** PVH axonal labeling (red fibers) surrounding cholinergic neurons (green, ChAT-ir) in the compact formation of the nucleus ambiguus (NAc), and lighter labeling caudally in the semi-compact formation (NAsc) as seen in the sagittal plane (case #2511). See area outlined in Figure 7 at Lateral 2.10 mm. Scale bar = 200 μm.

(**B**) PVH axonal labeling surrounds some of the tyrosine-hydroxylase containing neurons in the C1/A1 transition zone (ice-blue) as seen in the sagittal plane. Image taken from area outlined in the Lateral 2.10 mm sagittal section shown in Figure 7. Scale bar = 100 μm.

(**C**) PVH axons distributed among the PNMT-immunoreactive (adrenergic, green) C1 neurons in the RVLM. See **D** for scale bar.

(**D**) PVH axonal labeling is clustered around some of the PNMT-immunoreactive neurons of the C1/A1 transition area (green). Scale bar = 100 μm.

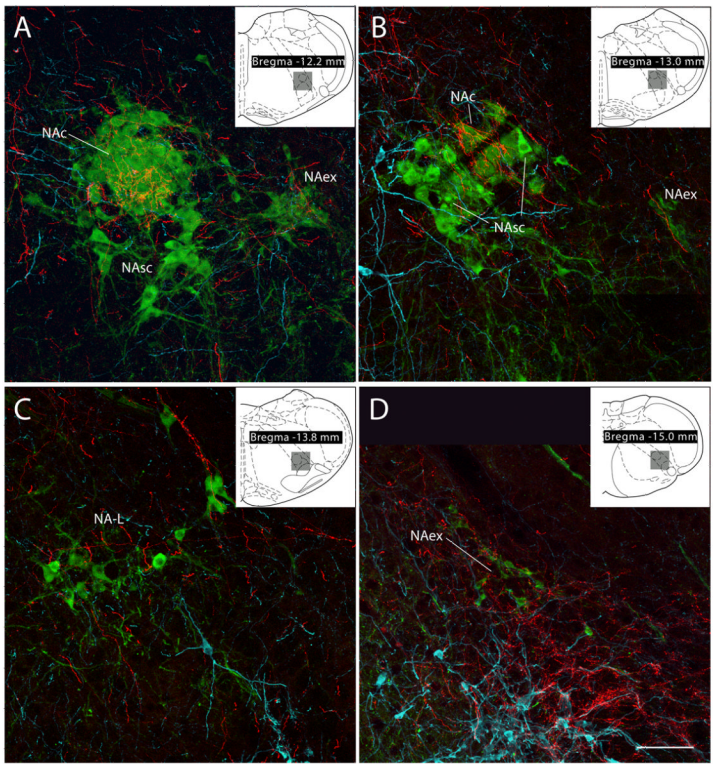


**Figure 9.**

Confocal montages showing PVH axons (red) in different subdivisions of the nucleus ambiguus (cases #2223 & #2221). ChAT-labeled cell bodies appear green. (**A**) & (**B**) Dense axonal labeling is seen in the nucleus ambiguus-compact subdivision (NAc), which contains esophageal motoneurons. A very weak input was seen in the nucleus ambiguus-subcompact subdivision (NAsc) which was noted in the sagittal section presented in Figure 8B. This area contains pharyngeal motoneurons. **A, B, & D:** Clusters of smaller ChAT-ir neurons lying outside the principal nucleus ambiguus cell column form a subdivision that has been termed the nucleus ambiguus-external formation (NAex). It contained moderate-to-dense concentrations of axonal varicosities. Neurons in this region are parasympathetic preganglionic vagal motoneurons. **C:** Laryngeal-related motoneurons in the nucleus ambiguus-loose formation (NA-L) receive a variable density of input from the PVH; most of these exhibit few or no apparent contacts, while others, such as the dendrite at the top of this panel, exhibited a dense innervation. **D:** Note also the denser labeling caudally surrounding the A1 noradrenergic neurons (TH-immunoreactive, show in ice-blue) and extending laterally into a functionally-defined region termed the CPA (described below). Scale bar = 100 μm.

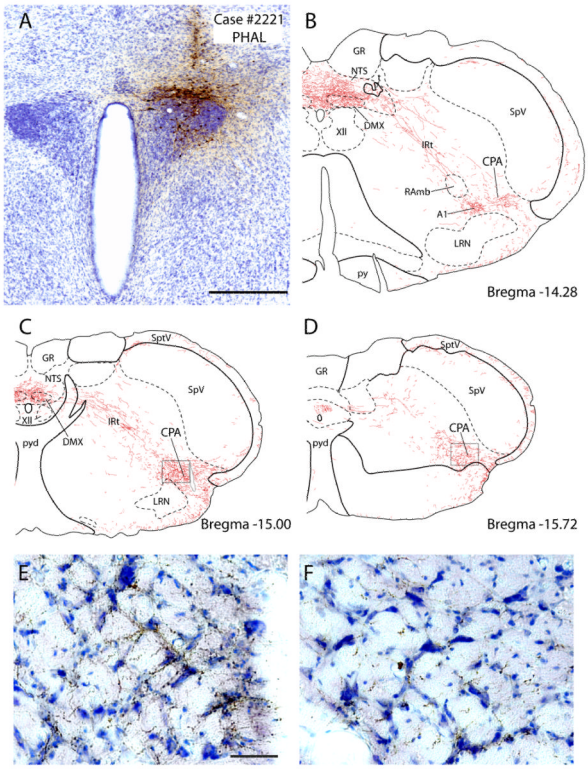


**Figure 10.**

The PVH densely projects to a region of the caudalmost part of the ventrolateral medulla known as the caudal pressor area (CPA). **A:** Axonal labeling is shown here in case #2221, which exhibited the densest axonal labeling in this region (in a distribution similar to that seen in other cases, including case #2223) after a PHAL injection centered in the dorsal parvicellular PVH. Scale bar = 500 μm. **B-D:** These drawings illustrate successively more caudal levels through the ventrolateral medulla beginning with (**B**) roughly the last medullary level shown from case #2223 (see Fig. 4 J) and extending through the pyramidal decussation (**C**-**D**). At the rostral end of the CPA (**B**), axonal labeling extended laterally from the caudal A1 noradrenergic neurons (the location of A1 was verified in adjacent sections labeled for TH+PHAL). The densest and most extensive axonal labeling was found in the mid-CPA at levels containing the pyramidal decussation (**C**), but a moderate density of axonal labeling continued through the end of the medulla (**D**) and into the lateral spinal nucleus and dorsolateral funiculus of the cervical spinal cord (not shown). In panel (**C**), the structure outlined in gray within the CPA is a blood vessel. **E & F:** Photoimages showing axonal labeling in the CPA from respective areas outlined in panels **C & D.** Scale bar = 100 μm.

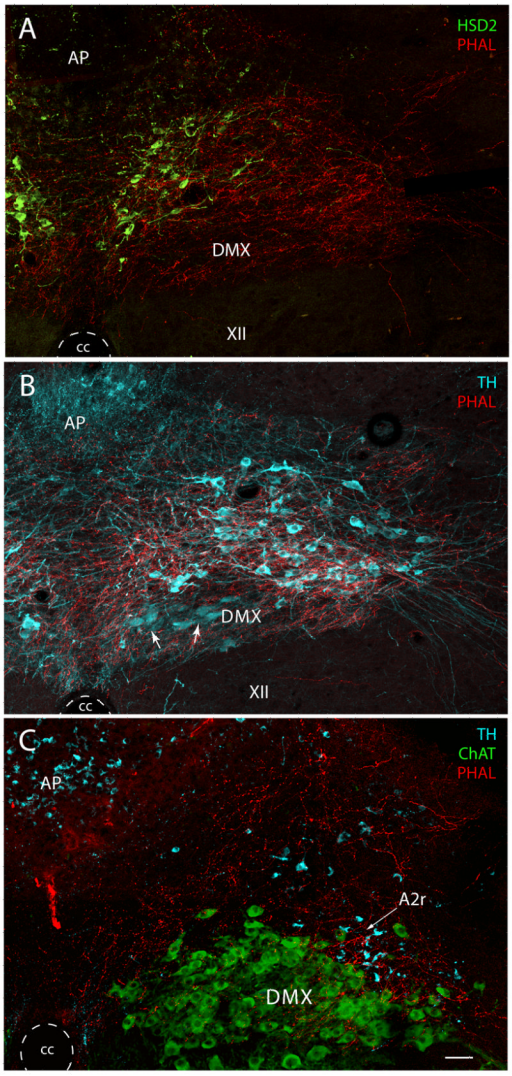


**Figure 11.**

These images compare axonal labeling in the dorsomedial medulla at the level of the area postrema with markers for established subpopulations of neurons in the NTS and dorsal vagal nucleus (DMX). (**A**) Aldosterone-sensitive NTS neurons (HSD2-ir, green) are situated along the medial border of the medial subnucleus of the NTS, amid a dense field of varicose axons from the PVH (PHAL-ir, red). This section contains the mid-caudal AP, which contained very little axonal labeling. (**B**) The A2 noradrenergic neurons (TH-ir, ice-blue) occupy a large extent of this dense field of PVH axon terminals. Note also the presence of dopaminergic neurons in the dorsal vagal nucleus (DMX) (arrows), with more diffuse TH immunoreactivity. Relative to the A2 neurons, these catecholaminergic vagal motoneurons receive very little input from the PVH. This section contains the caudal AP, which contains very little axonal labeling relative to the underlying NTS. **C:** Dense PVH projection to the rostralmost A2 noradrenergic neurons (A2r), which lie along the rostral, dorsolateral edge of the dorsal motor nucleus of the vagus (DMX). At first glance, this dense terminal field appeared to target the lateral DMX (ChAT-ir, green), but upon closer inspection in every case, this dense concentration of PVH axonal labeling appears to target the dendrites and somata of A2r neurons, while only a moderate density of terminals targets neighboring and intermingled neurons in the DMX, all of which are ChAT-ir. This section contains the

rostralmost AP, which exhibits minimal axonal labeling. Panels (A) and (B) were taken from case #2223 (Figs. 2 &3 for injection site), while (C) was taken from case #2276 (injection site not shown). Scale bar = 50 μm.

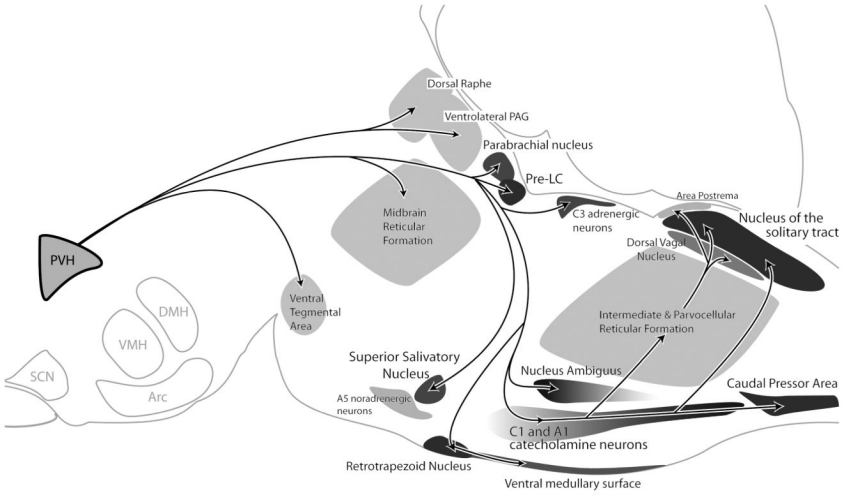


**Figure 12.**

Summary diagram showing the major brainstem sites innervated by the PVH. Individual areas are represented schematically in their approximate positions, and darker shading indicates a qualitatively denser projection from the PVH.

**Table 1**

PVH projections to various nuclei in the brainstem differed in some respects between the present investigation and previous reports, generally reflecting the greater level of detail provided here. This list is based on data provided in a previous PHAL anterograde tracing study (Table 1 of Zheng et al., 1995). Qualitative labeling data from the Zheng et al. study ("+/++/+++") were copied directly from their table, and our results were classified as follows (adapted from Zheng et al., 1995). Based on visual examination of PHAL axonal labeling in tissue sections from the cases shown here, "0" = zero or extremely few potential boutons or varicose axons; "0/+" = sparse boutons or axonal varicosities which could target an occasional neuron in the target nucleus; "+" lightly scattered boutons and/or varicose axons; "++" moderately dense boutons and varicose axons; "+++" dense axon terminal field, with abundant branches and boutons over a majority of the target region. Besides the Zheng et al. study, other PVH tracing studies did not provide a comparison table. Thus, we categorized the findings reported in other studies using similar criteria: "+++" was used for qualifiers such "dense network" and "strongly branch and terminate"; "++" for adjectives like "some" varicosities; and "+" for qualifiers such as "minor" or "a small number of" (examples quoted from Saper et al., 1976;Swanson, 1977;Luiten et al., 1985). Note that these inherently subjective designations are intended to represent the written interpretations provided in each article, not our re-interpretation of data from their figures that did not receive comment in their manuscript; brainstem regions not specifically mentioned in their text or highlighted in their figures were left blank.

| | Present data | Zheng et al. 1995[1] | Toth et al. 1999[1] | Luiten et al. 1985[1] | Swanson 1977[2] | Saper et al. 1976[3] |
|---|---|---|---|---|---|---|
| **Midbrain periaqueductal gray matter (PAG)** | | ++/+++ | | ++ | + | |
| **PAGd** | 0/+ | | | | | |
| **PAGdL** | 0/+ | | | | | |
| **PAGL** | + | | | | | |
| **PAGvL** | ++ | | | | | |
| **PAGv** | + | | | | | |
| **Edinger-Westphal nucleus** | 0/+ | + | | + | + | |
| **Interfascicular nucleus** | 0/+ | +/++ | | | | |
| **Ventral tegmental area** | +/++ | | | | | |
| **Rostral linear raphe** | + | +/++ | | | | |
| **Pedunculopontine nucleus** | ++ | ++/+++ | | +++ | | |
| **Mesencephalic reticular formation** | ++ | | | | | |
| **Dorsal raphe (including A10dc group)** | ++ | +/++ | | ++ | | |
| **Median raphe** | + | +/++ | | ++ | | |
| **Nucleus of the lateral lemniscus** | 0 | ++/+++ | | 0 | | |
| **Kölliker-Fuse nucleus** | 0/+ | | | | | |
| **Parabrachial nucleus** | | ++ | | ++ | + | |
| **PB lateral crescent/dorsal lateral** | + | | | | | |
| **PB superior lateral** | + | | | | | |

| | Present data | Zheng et al. 1995[1] | Toth et al. 1999[1] | Luiten et al. 1985[1] | Swanson 1977[2] | Saper et al. 1976[3] |
|---|---|---|---|---|---|---|
| **PB central & dorsal lateral (caudal-middle)** | ++ | | | | | |
| **PB central & dorsal lateral, rostral** | + | | | | | |
| **PB external lateral, caudal-middle** | ++ | | | | | |
| **PB external lateral, rostral** | + | | | | | |
| **PB medial-central** | + | | | | | |
| **PB waist** | ++ | | | | | |
| **PB medial-dorsomedial** | +++ | | | | | |
| **Locus coeruleus** | 0/+ | ++ | +++ | ++ | + | |
| **Pre-locus coeruleus** | +++ | | | | | |
| **Barrington's nucleus (pontine micturition center)** | 0 | | ++ | | | |
| **Raphe magnus** | + | +/++ | | ++ | | |
| **Raphe pallidus** | + | +/++ | | ++ | | |
| **C3 adrenergic neurons** | ++ | | | | | |
| **Superior salivatory nucleus** | +++ | | | | | |
| **A5 noradrenergic neurons** | + | | | | | |
| **Ventral medullary surface (including RTN)** | +++ | | | | | +++ |
| **Nucleus ambiguus** | | + | | ++ | + | + |
| **NA compact formation** | +++ | | | | | |
| **NA semi-compact formation** | + | | | | | |
| **NA loose formation** | + | | | | | |
| **NA external formation** | ++ | | | | | |
| **Lateral paragigantocellular nucleus (RVLM)** | | +/++ | | | | |
| **Rostral C1 neurons** | +/++ | | | | | |
| **C1-A1 transition region** | +++ | | | | | |
| **Dorsal motor nucleus of the vagus** | ++/+++ | ++/+++ | +++ | +++ | + | +++ |
| **Area postrema** | + | + | | + | | |
| **Nucleus of the solitary tract** | | ++/+++ | | +++ | | |
| **Rostral NTS -- central & lateral (gustatory)** | 0 | | | | | |
| **Rostral medial NTS (including C2 neurons)** | ++ | | | | | |
| **Intermediate NTS at 4th ventricle** | + | | | | | +++ |
| **Dorsomedial NTS** | ++/+++ | | | | | |

| | Present data | Zheng et al. 1995[1] | Toth et al. 1999[1] | Luiten et al. 1985[1] | Swanson 1977[2] | Saper et al. 1976[3] |
|---|---|---|---|---|---|---|
| **Gelatinous NTS** | +/++ | | | | | |
| **Parvicellular NTS** | ++/+++ | | | | | |
| **Periventricular Zone at 4th Ventricle** | +++ | | | | | |
| **Central (esophageal sensory) NTS** | 0/+ | | | | | |
| **Medial NTS at area postrema (including A2 neurons)** | +++ | | +++ | | | |
| **Subpostremal NTS** | ++ | | | | | |
| **Commissural NTS (including A2 neurons)** | +++ | | +++ | | | +++ |
| **Interstitial and Ventrolateral NTS** | 0/+ | | | | | |
| **Intermediate reticular formation** | ++ | | | | + | + |
| **Parvocellular reticular formation** | +/++ | | | ++ | | |
| **Spinal trigeminal nucleus (lamina I & paratrigeminal n.)** | + | +/++ | | | | |
| **Lateral reticular nucleus** | 0 | +/++ | | ++ | | |
| **Caudal ventrolateral medulla** | | | +++ | | | |
| **A1 neurons** | +++ | | | | | |
| **Caudal pressor area** | +++ | | | | +* | |

[1] PHAL anterograde tracing

[2] Oxytocin-immunoreactive axon labeling

[3] 3H-amino acid anterograde tracing (large injection site involving the caudal-lateral PVH and a large expanse of the LHA and ZI)

* Before the CPA was identified, Swanson described labeling in the lateral tegmental field & dorsal part of the lateral funiculus